

Lilla Roszik

The BiP Chaperone from the Endoplasmic Reticulum of Zebrafish (*Danio rerio*) and Golden Hamster (*Mesocricetus auratus*)



UNIVERSIDADE DO ALGARVE

Faculdade de Ciências e Tecnologia

2025

Lilla Roszik

**The BiP Chaperone from the Endoplasmic Reticulum of
Zebrafish (*Danio rerio*) and Golden Hamster
(*Mesocricetus auratus*)**

Mestrado em Biologia Marinha

Supervisor:

Eduardo Pinho Melo



UNIVERSIDADE DO ALGARVE

Faculdade de Ciências e Tecnologia

2025

Abstract

The Hsp70 family of molecular chaperones plays a crucial role in maintaining cellular proteostasis by promoting protein folding, transport, and degradation. One of its component proteins, the binding immunoglobulin protein (BiP), is an essential endoplasmic reticulum chaperone required for proper protein folding and stress response.

The primary objective of this work was to clone the open reading frame of the BiP gene from zebrafish (*Danio rerio*), a model organism that is frequently used to study the molecular and genetic causes of human disorders. More than 70% of the genes between humans and zebrafish are similar, including many orthologs connected to neurodegenerative illnesses like Alzheimer's.

For the sake of further functional investigations, the open reading frame of the zebrafish BiP gene was amplified and inserted into a bacterial expression vector. From zebrafish, the total RNA of caudal cell lines was extracted and reverse transcribed to create complementary DNA. The target DNA sequence was amplified by polymerase chain reaction (PCR) using specific primers for BiP. The golden hamster BiP ORF was removed from the backbone pQE10, and the amplified product was cloned into the vector. After transforming the recombinant plasmid into *Escherichia coli* DH5 α for propagation and isolation, the insertion of the open reading frame of zebrafish BiP was sent to sequencing. Unfortunately, *E. coli* recombines the zebrafish BiP ORF, contrary to the golden hamster ORF previously cloned into the same vector. Different *E. coli* strains deficient in DNA recombination should be tested soon.

This work aimed to establish the foundation for further investigations into the activity and biochemical characteristics of zebrafish BiP and its interactions with co-chaperones and client proteins in comparison with the mammalian BiP from golden hamster. At the longer term, we want to understand how the chaperone machinery of the endoplasmic reticulum has evolved in resolving protein aggregates associated with neurodegenerative diseases.

Keywords: Hsp70 family, BiP (Binding Immunoglobulin Protein), Zebrafish (*Danio rerio*), Golden hamster (*Mesocricetus auratus*), protein misfolding, neurodegenerative diseases

Resumo

As células possuem um conjunto de proteínas, designadas chaperones moleculares, absolutamente essenciais para assegurar a síntese de proteínas funcionais, responder a condições de stress que afetam a integridade do proteoma e direcionar proteínas danificadas para os mecanismos de reciclagem celular como o lisossoma e o proteassoma. A família de chaperones moleculares Hsp70 é das mais relevantes, desempenhando um papel crucial na manutenção da homeostase do proteoma celular (também designada proteostase). Um dos membros dessa família, o chaperone BiP (binding immunoglobulin protein), é essencial no retículo endoplasmático, a chamada via secretória das células, onde cerca de 20% do proteoma é sintetizado. Tem um papel fundamental no “folding” das proteínas no retículo endoplasmático e na resposta ao stress celular resultante do “misfolding” e agregação proteica que está associada à morte das células neuronais (neurodegeneração) em várias patologias como por exemplo a doença de Alzheimer. Em 2022, descobriu-se que a BiP, para além da função clássica de chaperone envolvido na catálise do folding de proteínas, possui a capacidade de desagregar proteínas no retículo endoplasmático (Melo et al., 2022). O estudo da capacidade da BiP para resolver agregados proteicos e impedir a sua acumulação no retículo endoplasmático é importante para perceber os mecanismos celulares que previnem a neurodegeneração e, eventualmente, desenvolver estratégias terapêuticas para tratamento das doenças neurodegenerativas.

O objetivo principal deste trabalho consistiu na clonagem da sequência codificante (designada “Open Reading Frame” – ORF) da BiP do peixe zebra (*Danio rerio*), num vetor adequado para expressão da proteína na bateria *Escherichia coli*. O peixe zebra é um organismo modelo, frequentemente usado para estudar as causas genéticas e moleculares de doenças humanas. Mais de 70% dos genes humanos e do peixe zebra são similares, incluindo muitos genes ortólogos relacionados com doenças neurodegenerativas. A ORF da BiP do peixe zebra foi amplificada e inserida num vetor para expressão da proteína na bactéria *E. coli*. A partir do ácido ribonucleico (RNA) total extraído de uma linha celular contínua isolada da cauda do peixe zebra, sintetizou-se a cadeia de ácido desoxirribonucleico complementar (cDNA) usando o enzima transcriptase reversa e “primers” com 18 nucleótidos timina e 6 nucleótidos aleatórios (“random hexamers”). O cDNA foi depois usado como molde, juntamente com primers específicos para a sequência alvo, para amplificar a ORF da BiP do peixe zebra pela reação de PCR (“polymerase chain reaction”). Nesta reação de PCR usou-se uma DNA polimerase à

prova de erro e, após otimização da temperatura de hibridação dos primers, conseguiu-se amplificar a ORF da BiP do peixe zebra. Para obter maiores quantidades desta ORF, usou-se o produto desta primeira reação de amplificação, após diluição adequada, como molde para nova reação de PCR, um procedimento frequentemente designado por “nested” PCR. Antes de avançar para a clonagem da ORF da BiP do peixe zebra num vetor adequado, mandou-se sequenciar o produto de PCR para confirmar a sequência alvo. Pela análise das sequenciações obtidas para as duas cadeias complementares de DNA, em comparação com a sequência esperada (gene ID 378848 e sequência referência NM_213058.1 do National Center for Biotechnology Information), confirmou-se que era efetivamente a ORF da BiP do peixe zebra. Confirmou-se 92% da sequência e verificou-se a presença de 9 mutações silenciosas e uma mutação que substituiu o aminoácido prolina por uma leucina, na posição 374 da BiP do peixe zebra. Para clonar esta ORF no vetor pQE10 desenhado para expressão de proteínas heterólogas em *E. coli* e com resistência ao antibiótico ampicilina, primeiro digeriu-se o vetor com os enzimas de restrição BamHI e AflIII para remover a ORF da BiP de hamster sírio, previamente clonada no vetor pQE10. Depois, a ORF da BiP do peixe zebra amplificada por PCR, foi também duplamente digerida com os mesmos enzimas de restrição cujas sequências de reconhecimento e corte estavam incluídas nos primers usados na amplificação. Por fim, procedeu-se à ligação do ORF ao vetor, usando o enzima DNA ligase T4. Após transformação de células de *E. coli* DH5 α competentes, obtiveram-se colônias que foram crescidas em meio líquido para isolamento do plasmídeo e posterior sequenciação. Inesperadamente, depois de sequenciar várias colônias, verificou-se que ocorre recombinação da ORF pelas células de *E. coli* DH5 α . Esta recombinação resulta da sequência da ORF da BiP do peixe zebra, visto que não ocorria quando a ORF inserida no vetor era a da BiP de hamster sírio. Para solucionar este problema, vai usar-se uma estirpe de *E. coli* alternativa à DH5 α , designada Stbl3 e recomendada para reduzir a frequência de recombinação homóloga.

Neste trabalho, efetuou-se ainda a expressão da ORF da BiP de hamster sírio previamente clonada no vetor pQE10 usando células de *E. coli* BL21(DE3) adequadas para expressão de proteínas heterólogas. Após expressão, a BiP de hamster sírio foi purificada por cromatografia de afinidade por metal imobilizado (IMAC – “Immobilized metal affinity chromatography”) e o grau de pureza após purificação analisado por electroforese em gel de poliacrilamida desnaturante (SDS_Page – “Sodium dodecyl sulfate polyacrylamide gel electrophoresis”).

A clonagem da ORF da BiP do peixe zebra tinha como objetivo estudar a função e o mecanismo da BiP de dois vertebrados evolutivamente distantes, o peixe zebra e o hamster sírio. Pretende-se no futuro, perceber se a evolução ao longo da linhagem dos vertebrados conduziu a uma BiP

mais eficiente na sua atividade de hidrólise de ATP (ATPase), na sua capacidade de catalisar o enrolamento correto de outras proteínas, na sua interação com outros co-chaperones importantes na manutenção da proteostase celular e, principalmente, na sua capacidade de resolver agregados proteicos resultantes do “misfolding” das proteínas. A longo prazo, pretende-se entender como é que a maquinaria de chaperones do retículo endoplasmático evoluiu para impedir/resolver a acumulação de agregados proteicos associados com doenças neurodegenerativas.

Palavras chave: família de proteínas Hsp70, chaperone BiP (“Binding Immunoglobulin Protein”), peixe zebra (*Danio rerio*), hamster sírio (*Mesocricetus auratus*), “misfolding” proteico, doenças neurodegenerativas

Declaração de autoria de trabalho

Declaro ser a autora deste trabalho, que é original e inédito. Autores e trabalhos consultados estão devidamente citados no texto e constam da listagem de referências incluída.

Declaração de direitos de autor

A Universidade do Algarve reserva para si o direito, em conformidade com o disposto no Código do Direito de Autor e dos Direitos Conexos, de arquivar, reproduzir e publicar a obra, independentemente do meio utilizado, bem como de a divulgar através de repositórios científicos e de admitir a sua cópia e distribuição para fins meramente educacionais ou de investigação e não comerciais, conquanto seja dado o devido crédito ao autor e editor respetivos

Acknowledgments

Above all, I would like first to express my most sincere gratitude to my supervisor, Professor Eduardo Pinho Melo, without whose invaluable guidance, expertise, encouragement, this journey would not have been possible. It has been my pleasure to learn so much under his mentorship, and I am grateful for the opportunity to have his support in my academic growth.

To Fernando, the best lab partner I could have ever had—thank you for your infinite patience and for always being willing to take the time to explain something to me when I needed it. Your support and your company have made every difficult moment in the lab easier and more enjoyable.

A very big thank you to my parents and my sister for the unconditional love, support, and faith they have given me, which have been my source of strength. I would like to take the opportunity to thank everyone who has ever loved me and always stood by my side no matter the distance or the obstacles.

Also want to say thank you to my boyfriend, Zoli, who is steadily on my side, and supporting me not just emotionally, but in the growth of my professional carrier.

To my best friends from Hungary- Fanni and Tamás, - I owe my success to your constant encouragement and support. Also thank you Bálint and Liza, my great friends from my home. All of your friendship has been a source of motivation and comfort to me, even when the miles between us. I am always grateful to have you by my side and believing in me.

I would like to express my deepest gratitude to my trainer and friend, Nagy Ferenc Gábor, for his unwavering support. Without his selfless help and constant presence in my life, completing this thesis would not have been possible.

Last but not least, my friends from the University of Algarve, thank you for all the unforgettable moments we have spent together and for the unwavering support you have given me during my studies. The amazing time we spent together, made this journey not only rewarding but also enjoyable.

I also want to dedicate this acknowledgment to Pirulito, my dog, and my loyal companion. I got Pirulito from Praia de Faro when I began my university studies and he has been with me

every day since. He has been a source of great joy and comfort and has been with me once daily throughout what has been the hardest time of this journey. Thank you, Pirulito, for being my source of unconditional love and always reminding me to find happiness in the simplest of things and for being my inspiration.

Table of contents

Abstract	ii
Resumo	iii
Acknowledgments	vii
1. Introduction	1
1.1. Recombinant DNA technology	1
1.2. Zebrafish as a Model Organism for human diseases	1
1.3. Chaperone Proteins	3
1.3.1. The Hsp70 family	4
1.3.1.1. The binding immunoglobulin protein BiP	6
1.3.1.2. Role of chaperones in Neurodegenerative diseases	10
2. Materials & methods.....	13
2.1 Preparing the competent <i>E. coli</i> DH5 α cells.....	14
2.2. Cloning of the open reading frame (ORF) of zebrafish BiP	15
2.3. Extraction of total RNA (tRNA).....	16
2.4. Synthesis of cDNA.....	16
2.5. PCR to amplify the ORF of zebrafish BiP	17
Extracting the amplicon from agarose gel.....	18
2.6 Nested PCR to amplify the ORF of zebrafish BiP	19
2.7. Double digestion of the backbone and insert.....	20
2.7.1. Double digestion of Bip vector.....	20
2.7.2. Double digestion of the PCR product	21
2.8 Ligation and transformation of <i>E. coli</i> DH5 α	21
2.8.1. Ligation	21
2.8.2. Transformation	22
2.9. Minipreps of the construct for zebrafish BiP	Hiba! A könyvjelző nem létezik.
2.10. Expression and purification of golden hamster (<i>Mesocricetus auratus</i>) BiP (haBiP) 24	
2.10.1 Transformation of <i>E. coli</i> BL21 (DE3)	24
3. Results and Discussion.....	26
3.1 Cloning the ORF of zebrafish BiP	26
3.1.1. PCR to amplify the ORF of zebrafish BiP	26
3.1.2. Nested PCR to amplify the ORF of zebrafish BiP	28

3.1.2 Backbone.....	35
3.1.3 Ligation and Transformation	37
3.2. Expression and Purification of hamster BiP	39
3.2.1.IMAC Purification (Immobilized Metal Affinity Chromatography).....	39
3.2.2. SDS page.....	40

List of figures

Figure 1.1 Primary and tertiary structure of Hsp70 showing the nucleotide binding domain (NBD), linker (L), substrate binding domain (SBD) including the lid (SBD lid) and the C-terminal domain (CTD). Hsp70 atomic structures in the closed (left structure) Hsp70 atomic structures in the closed (left structure PDB 2KHO) and open (right structure PDB 4JNE) conformations. NBD subdomains are referred to as IB, IIB, IA, and IIA. (Fernández-Fernández & Valpuesta).....	6
Figure 1.2 Close and Allosteric Opening of the Polypeptide-Binding Site in a Human Hsp70 Chaperone BiP (Yang et al., 2015).....	8
Figure 1.3 Amyloid disaggregation model using the Hsp70 chaperone apparatus. DNAJB1 uses multivalent contacts with the flexible C-terminal tails to specifically identify oligomeric α -synuclein. DNAJB1 uses several recruiting cycles to encourage the high-density loading of Hsp70 on the amyloid surface. Hsp110 preferentially dissociates Hsp70 that have not been grouped by DNAJB1 because of its large molecular mass. To provide entropic pulling forces that destabilize the amyloid fibril and cause fibril fragmentation and/or monomer extraction, this activity biases the positioning of Hsp70 to the most productive sites. Throughout multiple Hsp70 chaperoning cycles, DNAJB1 can stay connected and sense the substrate's oligomeric state. Either "T" for ATP or "D" for ADP denotes the nucleotide status of Hsp70 and Hsp110.	12
Figure 2.1 shows the map for the vector haBiP_27-654_pQE10 that we have used as the backbone after removing hamster BiP as the insert to be replaced by zebrafish BiP. We were planning on cloning between BamH1 and AflIII.	15
Figure 3.1 On this figure, the cDNA can be seen amplified with PCR. We were expecting a band with a size of 2000 bp.	28
Figure 3.2 Nested PCR product where Sample1, Sample 2 are PCR product diluted to 1:10; Sample 3, Sample 4 are PCR product diluted 1:100.	290
Figure 3.3 Shows the four single, and one double digestion of the BiP vector. Sample 1. Bspt1+ Buffer Tango; Sample 2. Bspt1+ Buffer O; Sample 3. BamH1+Buffer Tango; Sample 4. BamH1+ Buffer BamH1+; Sample 5. Bspt1 + BamH1 + Buffer Tango.....	38
Figure 3.4 Double digested backbone with the restriction enzymes. Sample 1, Sample 2, and Sample 3 contain BamH1 and Bspt1 endonucleases with buffer Tango.	39
Figure 3.5 BiP Chromatogram showing the Flow-through Peak, Elution Peak.	392

1. Introduction

2.9.Recombinant DNA technology

Following the cloning of a complete bacterial gene (Chang & Cohen, 1974), the development of heterologous recombinant gene expression technologies was marked by the finding that DNA from one species can be cloned and replicated in another. In the late 1960s, Hamilton Smith and Daniel Nathans identified the first restriction endonuclease (Smith, 1979). The discovery of the enzyme DNA ligase in 1967 by Martin Gellert made it possible to combine DNA molecules from various sources to create recombinant DNA molecules by covalently joining their ends with phosphodiester linkages (Bedows, 1977). The groundbreaking discovery of PCR in the 1980s, which amplified DNA fragments *in vitro*, paved the way for the creation of complex cloning techniques. Another significant development in molecular biology during the past ten years has been the routine synthesis of large DNA fragments of a particular sequence, which has become widely available and reasonably priced (Morrow et al., 1974).

2.10. Zebrafish as a Model Organism for human diseases

About 450 million years ago, the human (tetrapod) lineage split off from the zebrafish (teleost-bony fish) evolutionary lineage (Kumar and Hedges, 1998). Since separating from the tetrapod lineage, teleosts seem to have experienced another cycle of genome duplication, which was followed by the loss of many of the duplicated genes (Catchen et al., 2011). Zebrafish (*Danio rerio*) are small, resilient freshwater fish originally from India. Initially, they served as a model organism for research on the development of vertebrates. Zebrafish allow for the simple and efficient manipulation of many genes at physiologically appropriate levels (Newman et al., 2012). Zebrafish are vertebrates and so more relevant to comprehending human biology than invertebrate models like *Drosophila melanogaster* and *Caenorhabditis elegans*.

In the past ten years, the zebrafish model has been used more and more to study a wide range of human illnesses (Lieschke and Currie, 2007). Zebrafish is widely regarded, as an excellent model organism in molecular biology for various reasons, among them is the fact that they have genetic similarity to humans. Zebrafish share approximately 70% of their genes with humans, and about 84% of genes associated with human diseases have orthologues in zebrafish (Crouzier et al., 2021). Because of their transparency, high fertility, relatively low cost of

maintenance, and the possibility to manipulate their genome, zebrafish are an important model organism for studying human diseases and genetic functions. Zebrafish embryos are practically transparent, which enables live observation and modification of the embryonic development. Within 24-48 hrs post fertilization, they mimic many organs and systems, making it a fast model for developmental biology studies. Research employing zebrafish has uncovered distinctive features of genes that have been challenging to discover in rodent models, including genes orthologous to those altered in familial Alzheimer's disease. Therefore, zebrafish has become an increasingly common model for studying Alzheimer's dementia, complementing research employing other species to help us fully comprehend the condition (Newman et al., 2014). Indeed, genes orthologous to human genes known to play a role in AD are found in zebrafish. While the *APPA* and *appb* genes are "co-orthologs" of human amyloid precursor protein (APP) (Musa et al., 2001), the *psen1* (Leimer et al., 1999) and *psen2* (Groth et al., 2002) genes are orthologs of human *PSEN1* and *PSEN2*, respectively.

Autosomal-dominant Early Onset Alzheimer Disease (ADEOAD), whose frequency is estimated to be 5.3 per 100,000 persons at risk, is caused by mutations and duplications in amyloid protein precursor (APP), presenilin-1 (PSEN1), and presenilin-2 (PSEN2) (Sherrington et al., 1995; Rogaev et al., 1995; Levy-Lahad et al., 1995; Sherrington et al., 1996). A percentage of early-onset Alzheimer disease (eoAD) has been linked to mutations in three genes: presenilin 1 (PSEN1), amyloid precursor protein (APP), and presenilin 2 (PSEN2) (Krüger et al., 2012). According to the Alzforum database, PSEN1 is the most often implicated gene, with 221 mutations identified as harmful (Campion et al., 1999). With 32 pathogenic variants recorded, APP is the second most often affected gene. Moreover, 19 distinct PSEN2 pathogenic mutations have been documented. The amyloid- β precursor protein, which is encoded by APP, is processed by the β -secretase and γ -secretase complex to produce the amyloid β (A β) peptide, a crucial step in the pathophysiology of AD. A series of processes leading to AD are indeed triggered by the A β peptide's aggregation in the brain's parenchyma. When it aggregates in the cerebro meningeal arteries, it causes cerebral amyloid angiopathy (CAA), which is often linked to AD and causes white matter abnormalities and recurrent hemorrhagic strokes. Presenilins, the catalytic subunit of the γ -secretase complex, are encoded by PSEN1 and PSEN2 (Haass et al., 2012; Campion et al., 2016).

The increased aggregation of the A β peptide in the brain's parenchyma is believed to result from AD-EOAD causative mutations through one of two mechanisms: either a more

aggregation-prone form of the A β peptide or an increase in the production of all A β species (such as APP duplications or APP mutations around the β cleavage site).

2.11. Chaperone Proteins

Correct cellular function depends on protein homeostasis, also known as proteostasis, which is the balance of protein synthesis, folding, trafficking, assembly, and degradation. Cells have evolved a variety of mechanisms to regulate this process under stress (Zuiderweg et al., 2017). A ubiquitous class of cellular proteins known as molecular chaperones facilitates other polypeptides' proper folding and in certain situations, their assembly into oligomeric structures, although they are not components of those final structures. Although known chaperones lack the steric information necessary for protein folding, they do prevent ineffective folding and assembly pathways that could otherwise serve as dead-end kinetic traps and result in the wrong structures (Ellis, 1990).

Chaperones are similar in that they can identify and bind foreign proteins, which stops them from aggregating randomly (Beissinger & Buchner, 1998). One of the most common groups of chaperones, the 70-kDa heat shock protein (Hsp70) family of molecular chaperones is highly conserved across all organisms. The Hsp70 family of proteins regulates all aspects of cellular proteostasis, including the folding of developing protein chains, the import of proteins into organelles, the retrieval of proteins from aggregation, and the formation of multiprotein complexes. When a nucleoside binds to an adenosine-5'-triphosphate (ATP)-dependent chaperone (such as GroEL, Hsp70, or Hsp90), the chaperone may undergo significant conformational changes that enable it to switch between high- and low-affinity states for the substrate proteins (Ellis, 1990). Through improving cell viability and aiding in the repair of protein damage, these chaperones increase organismal survival and longevity in the face of proteotoxic stress. Extracellular Hsp70s play multiple cytoprotective and immunomodulatory functions. The last role can be chaperonins or stimulators of innate immune responses, or to facilitate the cross-presentation of immunogenic peptides through major histocompatibility complex (MHC) antigens. All of the physiological actions of Hsp70s depend on their ATP-regulated ability to bind with exposed hydrophobic surfaces of proteins. During the folding of polypeptides, ATP hydrolysis and the exchange of adenosine diphosphate (ADP) with ATP are essential processes for substrate binding and Hsp70 release. Hsp70 co-chaperones are a group of proteins that bind to different Hsp70 subdomains and

subsequently alter the chaperone's function (Radons, 2016). The chaperone machinery of the endoplasmic reticulum (ER), a site responsible for the manufacturing of about one-third of the cell's protein repertoire (including disease determinants, e.g. APP) is relevant to understand how cells deal with proteotoxicity resulting from protein misfolding and aggregation of secretory proteins. As newly generated proteins are translocated into the endoplasmic reticulum, the chaperone binding immunoglobulin protein (BiP), which is an Hsp70 molecular chaperone situated in the ER lumen, binds them and keeps them in a state suitable for further folding and oligomerization. BiP also participates in the retrograde transport of abnormal proteins intended for proteasomal degradation across the ER membrane and is a crucial part of the translocation process (Multhoff et al., 1995; Multhoff & Hightower, 1996; Hantschel et al., 2000; Gehrman et al., 2005).

1.1.1. The Hsp70 family

Hsp70 is a nanomachine that aids in protein folding by utilizing conformational changes driven by ATP hydrolysis. The common domain structure of Hsp70s, (Flaherty et al. 1990) is composed of a 44-kDa N-terminal nucleotide-binding domain (NBD) that binds and hydrolyzes ATP, a middle domain with protease-sensitive sites, and a 28-kDa C-terminal substrate-binding domain (SBD) that binds extended polypeptides (Figure 1.1). The ATP-binding pocket is surrounded by four subdomains (IA, IB, IIA, and IIB) that make up the nucleotide-binding domain (Flaherty et al. 1990). The SBD is separated into a C-terminal α -helical subdomain (SBD α), which functions as a flexible lid, and an N-terminal β -sheet (SBD β) domain (Zhang, Hong, & et al., 2023).

Stable misfolded or aggregated proteins can be recognized by Hsp70s thanks to their unfoldase activity, which also allows the proteins to unfold and spontaneously refold into natively refoldable species (Sharma et al. 2010). Together with dimeric co-chaperone Hsp40 and nucleotide exchange factors (NEFs), Hsp70 recognizes stable misfolded polypeptides. These proteins undergo repeated cycles of binding, ATP-dependent unfolding, and spontaneous refolding to become native proteins. The N-terminal nucleotide-binding domain of Hsp70 is a V-shaped structure made up of two subdomains (lobes) that envelope the ATP-binding site. The NBD and the SBD interact allosterically in the function of Hsp70. The SBD undergoes conformational changes driven by the NBD, while the NBD interface receives substrate-

induced conformational changes from the SBD (Zhuravleva & Gierasch, 2015; Taylor et al., 2018).

The accessibility of hydrophobic regions on proteins, which are typically hidden in the protein core, indicates a misfolded state on client proteins. There are two possible conformations for the SBD: open and closed. ATP interaction to the NBD causes the SBD open conformation, which has a poor affinity for client protein binding. The closed conformation is driven by ATP hydrolysis; structural changes start at the NBD and are transferred through the linker to cause the SBD base and lid subdomains to converge and bind to the client protein with high affinity. In the open conformation, the flexible and conserved linker makes contact with the NBD, and in the closed conformation, it separates from it.

J-protein (Hsp40) co-chaperones raise the basal ATPase activity of Hsp70 proteins, which are typically modest. In addition to binding client proteins to Hsp70, J-proteins also promote ATPase activity and effective client protein locking (Mayer & Bukau, 2005; Kampinga & Craig, 2010).

Another group of co-chaperones called the nucleotide exchange factors (NEFs) are responsible for ADP dissociation, which is necessary for the client protein to be released. Therefore, NEFs promote ADP/ATP exchange, inducing the open conformation, while J-proteins cause ATP hydrolysis, and enhance the closed conformation.

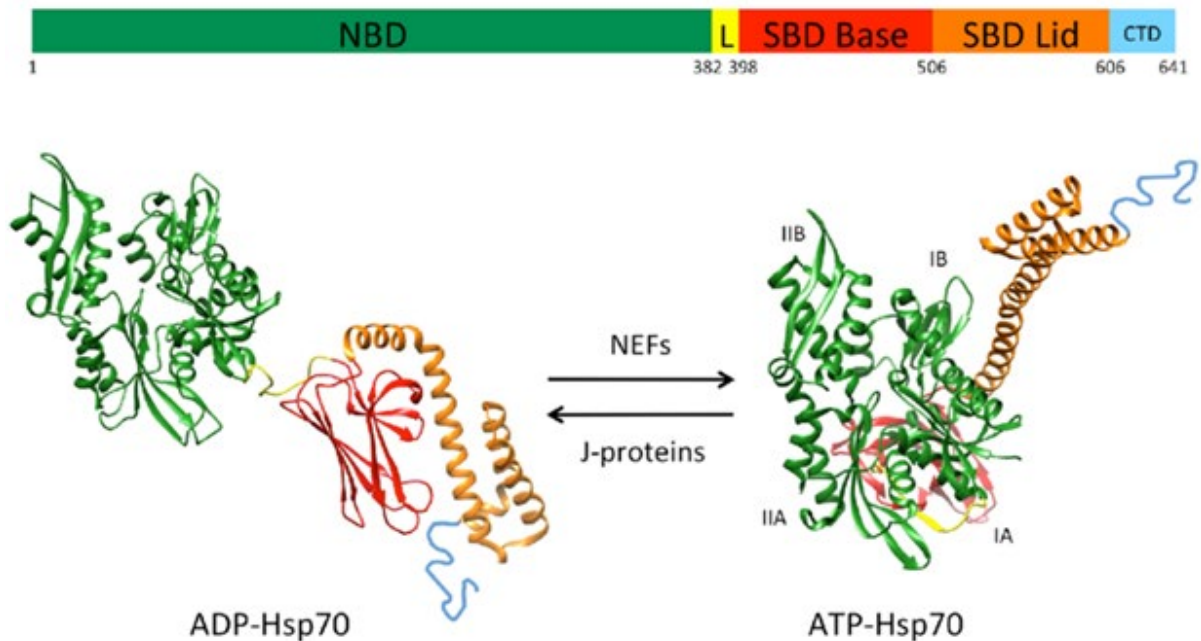


Figure 1.1 Primary and tertiary structure of Hsp70 showing the nucleotide-binding domain (NBD), linker (L), substrate-binding domain (SBD) including the lid (SBD lid) and the C-terminal domain (CTD). Hsp70 atomic structures in the closed (left structure PDB 2KHO) and open (right structure PDB 4JNE) conformations. NBD subdomains are referred to as IB, IIB, IA, and IIA. (Fernández-Fernández & Valpuesta, 2018). The role of nucleotide exchange factors (NEFs) and J-proteins co-chaperones on the equilibrium between the ADP- and ATP bound state is shown by the arrows.

Hsp70s are powerful anti-apoptotic proteins that prevent apoptosis on several levels. Hsp70 inhibits the assembly of the death-inducing signaling complex (DISC) (Guo et al. 2005b) and, on the other hand, prevents mitochondrial translocation and activation of Bax, which stops mitochondrial membrane permeabilization and the release of pro-apoptotic factors (Stankiewicz et al., 2005; Er et al., 2006).

1.1.1.1. The binding immunoglobulin protein BiP

BiP was first discovered on its own as the glucose-regulated protein Grp78 and as the immunoglobulin heavy chain binding protein. When it was established that BiP is the Hsp70 molecular chaperone family member that is found in the ER, its role as a broad specificity

molecular chaperone became evident. BiP is essential to every organism's biology, as evidenced by its great conservation across species. BiP functions as a molecular chaperone that aids in protein folding, import into the ER, protein elimination through endoplasmic reticulum associated degradation (ERAD), and Ca^{2+} homeostasis regulation. When proteins are misfolded, under glycosylated, or unassembled and their transport out of the ER is inhibited, BiP binds to these proteins temporarily. Furthermore, BiP inhibits apoptosis and promotes autophagy by activating the UPR pathway. BiP's links to cancer, cardiovascular illness, neurological disease, metabolic disease, autoimmune disease, and infectious disease demonstrate how frequently ER stress triggers these processes (Pouyssegur et al., 1977; Munro & Pelham, 1986).

The interaction of BiP's functions in autophagy, apoptosis, and unfolded protein response (UPR) needs more research to comprehend how BiP contributes to cell survival in response to ER stress and other illness situations. Drugs that target BiP have shown encouraging results in recent trials, especially in improving some cancer treatments and possible concurrent heart failure. These studies can be broadened to find novel chemical inhibitors and inducers of BiP to treat other pertinent disorders (Wang et al., 2017).

Unlike other Hsp70 proteins, BiP does not interact with native polypeptides. By identifying unfolded polypeptides and preventing intermolecular aggregation, BiP promotes the folding and assembly of newly synthesized proteins by keeping them in a state that allows for further folding and oligomerization. BiP three-dimensional structure has two major domains, just like other Hsp70 proteins: a C-terminal substrate-binding domain and an N-terminal domain containing the ATPase catalytic site (Figure 1.2.). The communication between these domains controls the duration and affinity of polypeptide binding (McKay, 1993). There is minimal interaction between the two domains in the nucleotide-free (apo) and ADP-bound states (Buchberger et al., 1995; Swain et al., 2007; Buchberger et al., 2008; Bertelsen et al., 2009). Similarly, to the isolated SBD, this state exhibits strong affinity for polypeptide substrates and delayed binding and release rates (Flynn et al., 1989; Schmid et al., 1994). While the resulting affinity is two to three orders of magnitude lower, the two domains are strongly linked in the ATP-bound state, leading to significantly faster kinetics in both binding and release of polypeptide substrates (Schmid et al., 1994).

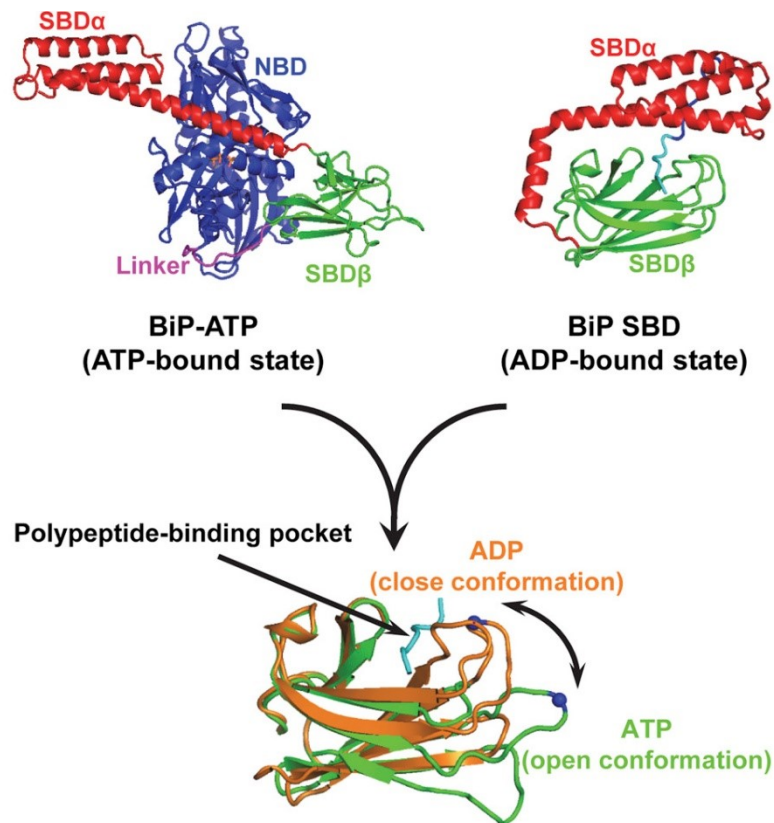


Figure 1.2 Close and Allosteric Opening of the Polypeptide-Binding Site in human Chaperone BiP (Yang et al., 2015)

The C-terminal domain's affinity for polypeptides is determined by the presence of ATP (low affinity but fast binding) or ADP (high affinity and sluggish exchange) in the nucleotide binding domain. The rate at which ATP is hydrolyzed by the N-terminal ATPase domain is accelerated upon polypeptide binding to the C-terminal domain. The nucleotide-binding domain (NBD) and substrate-binding domain (SBD) take on an open conformation when bound to ATP, which promotes substrate release. On the other hand, the polypeptide-binding pocket's close conformation is induced by the ADP-bound state, stabilizing the substrate association (Figure 1.2). As referred, effective chaperone function of BiP depends on the ATP-induced allosteric coupling (Mayer and Bukau, 2005). Therefore, cycles of binding and release of an unfolded polypeptide chaperoned by BiP can occur; the length of these cycles is determined by the rate at which BiP undergoes adenine nucleotide exchange of ATP for ADP and ATP hydrolysis. The polypeptide will interact with the chaperone until it no longer exhibits any BiP-binding motifs, but each time it is released, it will have the chance to advance down the folding pathway (McKay, 1993).

The nucleotide is bound in a deep cleft between the two lobes that make up the ATPase domain, which is made up of four subdomains. It is easy to map the amino acid sequence of the N-terminal domain of BiP onto the backbone of the Hsp70 structure. This indicates that the two proteins have extremely comparable conformations. The amino acid sequence of BiP shares 66% identity and 81% similarity with that of the cytosolic Hsp70 protein. The new fold found in the C-terminal substrate binding domain of *E coli* DnaK is probably shared by all members of the Hsp70 protein family, including BiP. It consists of a compact β -sandwich followed by helical elements. The beta sandwich is arranged in two sheets with four antiparallel beta strands in each, and the peptide is bound in an extended conformation in a channel formed by loops that connect strands of the sandwich. Binding of ATP to the N-terminal domain causes the lid to open, while hydrolysis of ATP to ADP results in a conformational change that causes the lid to close, encapsulating the peptide in the channel (Zhu et al., 1996).

BiP's capacity to distinguish between correctly folded and unfolded structures and to identify a broad range of polypeptides with no discernible sequence similarity is essential to its function as a generic chaperone in the ER lumen. Short synthetic peptides can interact with BiP *in vitro*, stimulating its ATPase activity and changing its oligomeric state upon engagement (Flynn et al., 1989; Blond-Elguindi et al., 1993a, 1993b; Fourie et al., 1994; Knarr et al., 1995; Chevalier et al., 1998; Carlsson & Lazarides, 1983; Leno & Ledford, 1990; Ledford & Leno, 1994). BiP, experiences a quick, reversible, and deactivating post-translational change. To match the supply of active BiP to the need for protein folding within the ER lumen, the post-translational covalent alteration works in tandem with the slower, traditional UPR. Now, it is known that this change is AMPylation of BiP's threonine 518, which was previously thought to be ADP-ribosylation and is catalyzed by the Ficdomain-containing protein (FICD) (Preissler et al., 2015; Perera & Ron, 2023; Freiden, Gaut, & Hendershot, 1992; Hendershot, Ting, & Lee, 1988; Leustek, Toledo, Brot, & Weissbach, 1991; Carlsson & Lazarides, 1983). In complexes with unfolded or unassembled polypeptides, only unaltered, monomeric BiP molecules are detected. Therefore, it would seem that post-translational modification of BiP creates a storage pool of BiP that may be called upon to return to the active form when necessary (Hendershot, Ting, & Lee, 1988; Freiden, Gaut, & Hendershot, 1992).

1.1.1.2. Role of chaperones in Neurodegenerative diseases

Aging-related impaired proteostasis is linked to a number of human illnesses. Highly ordered fibrillar-type protein aggregates are deposited into inclusion bodies in Parkinson's disease and other neurodegenerative diseases. The cellular protein quality-control machinery finds it challenging to handle these amyloid fibril aggregates due to their high stability (Kampinga & Bergink, 2016; Wentink et al., 2019).

Molecular chaperones are crucial for maintaining proteostasis; specifically, the chaperone heat shock protein 70 family is crucial for the folding, disaggregation, and degradation of proteins (Zuiderweg et al., 2017). ER stress has been implicated in the pathophysiology of neurodegenerative diseases in several studies (Ni & Lee, 2007). Huntington's disease and cerebral infarction are two conditions linked to cerebellar ataxia in which BiP is crucial. BiP has been demonstrated to bind to huntingtin aggregates in the Huntington's disease model and inhibit huntingtin aggregation at elevated doses (Muchowski et al, 2000). Consequently, cells that share both reduced BiP availability and mutant huntingtin exhibit hypersensitivity to ER stress (Lajoie & Snapp, 2011).

By repairing misfolded proteins, BiP reduces neuronal cell death brought on by ER stress in Marinesco-Sjögren syndrome, which is typified by cerebellar ataxia (Zhao et al., 2005; Anttonen et al., 2005). BiP expression is downregulated in cells with mutations that cause spinocerebellar ataxia type 17 (Lee et al., 2009). Through BiP-induced neuroprotective pathways, 2-deoxy-D-glucose therapy has been proposed to lessen brain injury in a mouse model of Parkinson's disease. By reprogramming ER stress signaling pathways to prevent apoptotic cell death, BiP overexpression was also reported to reduce α -synuclein cytotoxicity in rat and SH-SY5Y cell models (Gorbatyuk & Gorbatyuk, 2013).

The most common type of dementia is Alzheimer's disease (AD). According to the World Alzheimer Report (2010), there were an estimated 36 million people with AD in 2010. In 2024, this number rose to 55 million people. By 2030, that number is expected to rise to 66 million. Alzheimer's disease is characterized by gradual memory loss. However, despair, delusions, hallucinations, violent behavior, and deterioration of speech and motor abilities are also characteristics of AD (Voisin & Vellas, 2009). Despite these obvious behavioral changes, it might be challenging to accurately identify AD in its early stages. The causes and processes of Alzheimer's disease have been widely studied using rodent models. We still don't fully grasp the molecular processes that cause neurodegeneration, even after

years of rigorous research using these models. Alzheimer's disease has been firmly linked to BiP chaperone dysfunction, among other chaperones (Booth et al., 2015b; Ni & Lee, 2007). BiP's chaperone function may save neurons already loaded with β -amyloid protein, a significant contributor to extracellular senile plaques in Alzheimer's disease (Zhao et al., 2005; Anttonen et al., 2005). BiP inhibitors may therefore work better if administered early in Alzheimer's disease (Booth et al., 2015a).

As shown in Figure 1.1, Hsp70 function, including that of BiP, depends on co-chaperones from the J-domain protein (JDP) and nucleotide exchange factor (NEF) families, which guarantee substrate specificity, control ATPase cycle progression, and govern interactions with other chaperone networks and degradation pathways. It is yet unknown, nevertheless, how different co-chaperones allow the Hsp70 machinery to carry out particular tasks and, in turn, why particular Hsp70 activities call for particular co-chaperone partners. Recently it was shown that produced fibrils of the presynaptic protein α -synuclein, which is linked to Parkinson's disease, can be dissolved *in vitro* by the human Hsp70 chaperone and its co-chaperones DNAJB1 and Hsp110 (Figure 1.3) (Duennwald, Echeverria, & Shorter, 2012; Gao et al., 2015). DNAJB1 directs Hsp70 to fibrils and uses multivalent contacts to detect the oligomeric form of α -synuclein. Instead of the amyloid core itself, Hsp70 and DNAJB1 engage with the fibril via the exposed, flexible amino and carboxy termini of α -synuclein. By enabling the loading of many Hsp70 molecules in a densely packed configuration at the fibril surface—perfect for the production of "entropic pulling" forces—DNAJB1 and Hsp110 work in concert to significantly speed up α -synuclein disaggregation. Beyond the traditional substrate targeting and recycling roles that are ascribed to these Hsp70 co-chaperones, DNAJB1 and Hsp110 work together to facilitate amyloid disaggregation, which actively and crucially contributes to the amyloid substrate's remodeling. Molecular understandings of the necessary conditions for amyloid disintegration could serve as the foundation for novel neurodegenerative treatment approaches (Mayer & Gierasch, 2019; Rosenzweig et al., 2019). By speeding up ADP dissociation, which leads to ATP binding and Hsp70 interconversion to an open conformation, the NEF Hsp110 encourages Hsp70 recycling. High disaggregation efficiencies require thus the presence of a NEF (Bracher & Verghese, 2015).

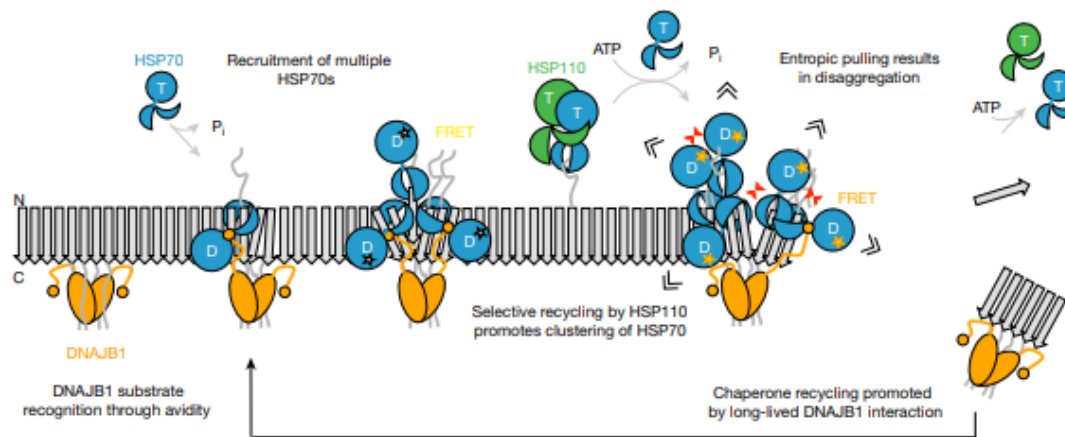


Figure 1.3 Amyloid disaggregation model using the Hsp70 chaperone apparatus. DNAJB1 uses multivalent contacts with the flexible C-terminal tails to specifically identify oligomeric α -synuclein. DNAJB1 uses several recruiting cycles to encourage the high-density loading of Hsp70 on the amyloid surface. Hsp110 preferentially dissociates Hsp70 that have not been grouped by DNAJB1 because of its large molecular mass. In order to provide entropic pulling forces that destabilize the amyloid fibril and cause fibril fragmentation and/or monomer extraction, this activity biases the positioning of Hsp70 to the most productive sites. Throughout multiple Hsp70 chaperoning cycles, DNAJB1 can stay connected and sense the substrate's oligomeric state. Either "T" for ATP or "D" for ADP denotes the nucleotide status of Hsp70 and Hsp110.

Several observations strongly support an entropic-pulling mechanism of amyloid disaggregation activity as described in Figure 1.3:

- (1) chaperone engages the fibrillar substrate by exposing disordered regions near the amyloid surface;
- (2) disaggregation necessitates Hsp70 crowding on the fibrils;
- (3) crowding has an energetic cost, which is partially covered by the affinity of JDP-mediated recruitment of Hsp70 to the fibrils;
- (4) Hsp110-specific activity encourages the selective reorganization of HSP70 proteins that are loaded ineffectively, favoring Hsp70 binding at high density where entropic-pulling effects are strongest;
- (5) the high molecular mass of the Hsp110 family is a crucial characteristic, confirming that excluded volume effects play a significant role in the disaggregation mechanism (De Los Rios et al., 2006; Sousa et al., 2016; Assenza et al., 2019).

The spread of protein aggregation linked to dementia may be slowed by chaperone-mediated amyloid disaggregation. However, potentially hazardous oligomeric species and fibril

fragments that could act as a template for more protein aggregation could also be produced during the disaggregation process (Pieri et al., 2012; Gao et al., 2015).

The objective of this work was to clone the ORF of BiP from zebrafish into an appropriate vector for expression in *E. coli* to compare its capability to disaggregate proteins with mammalian BiP from golden hamster. By comparing the activity of BiP to disaggregate proteins from two distant vertebrate clades, warm-blooded mammals and cold-blooded fish, we aim to understand how the chaperone machinery from the endoplasmic reticulum has evolved to maintain proteostasis and prevent neurodegeneration.

2. Materials & Methods

2.1 Preparing the competent *E. coli* DH5 α cells

The TB Buffer (100 mL) must be prepared sterile, using a 0.2 μ m filter before beginning the entire procedure of preparing competent *E. coli* DH5 α cells.

The components are listed below:

- 10 mM PIPES
- 15 mM CaCl₂
- 250 mM KCl
- 55 mM MnCl₂ (only add at the end after adjusting the pH)

The pH was adjusted to 6.7 with KOH.

The protocol to prepare the competent *E. coli* DH5 α cells was the following:

On the 1st Day: The *E. coli* strain needed to be grabbed from the -80 °C Ark. After plating, let it grow overnight at 37 °C. Inoculating a colony in 5 mL of LB took place on the 2nd Day and let it grow overnight at 37 °C (Pre-inoculum). On the 3rd Day: In the afternoon, inoculate 250 mL of LB (in 1 L Erlenmeyer flask) with 1 mL of pre-inoculum and let it grow overnight at 18 °C. The optical density (OD) was measured at 600 nm in a sample diluted 1:10 with water. On Day 4: Keep measuring the OD at 600 nm (sample diluted 1:10 with water), until an OD of 0.4 was obtained.

In the afternoon, the following steps were taken:

1. The Erlenmeyer flask was kept on ice for 10 minutes.
2. The culture was transferred to 5 sterile falcons (50 mL each) and centrifuged at 2500 g, at 4 °C, for 10 minutes. (Pre-cool the centrifuge)
3. The pellet of each falcon was resuspended in 16 mL of cold TB Buffer and kept on ice for 10 minutes.
4. Centrifuged the falcons at 2500 g, at 4 °C, for 10 minutes. (Pre-cool the centrifuge)
5. The pellet was resuspended in each falcon with 4 mL of cold TB Buffer and 280 μ L of 7% DMSO was gently added. Falcons then were kept on ice for 10 minutes.
6. Aliquots of 100 μ L were made in sterile Eppendorf and flash-freeze in liquid nitrogen or using dry ice.

7. The competent cells needed to be stored at -80 °C.

2.2. Cloning of the open reading frame (ORF) of zebrafish BiP

Figure 2.1 below shows the vector map containing the ORF of golden hamster BiP where the ORF of zebrafish BiP will be cloned replacing the hamster BiP.

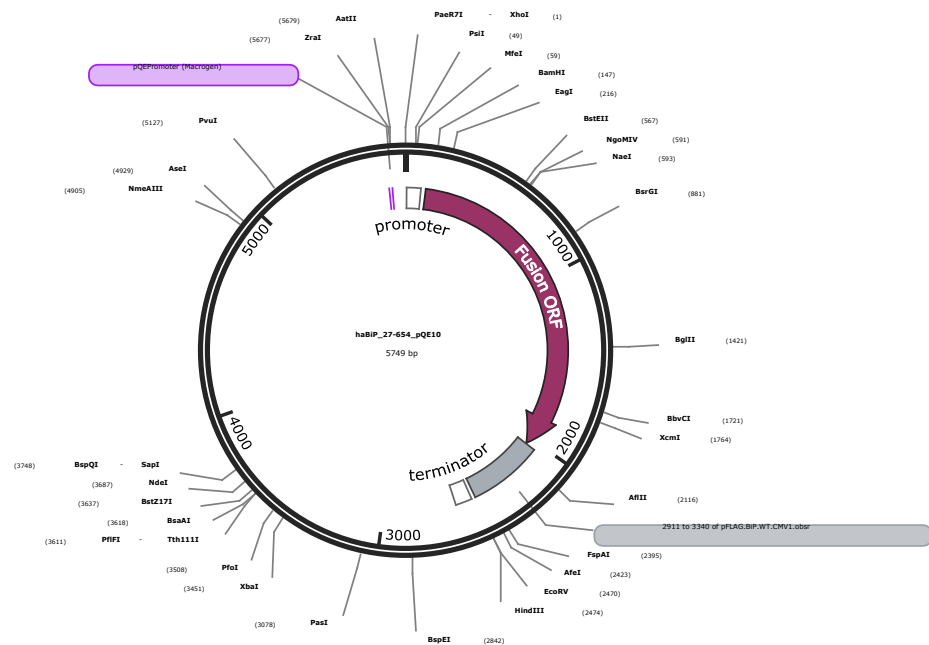


Figure 2.1. Shows the map for the vector haBiP_27-654_pQE10 that we have used as backbone after removing hamster BiP as insert to be replaced by zebrafish BiP. We planned the cloning between BamHI and AflIII that keeps the His tag on the vector for affinity purification.

Amplifying the open reading frame (ORF), and putting it into an appropriate vector for expression are the processes involved in cloning the zebrafish BiP ORF. The first step was to identify the zebrafish BiP (Uniprot Q7SZD3) ORF sequence using the database National Center for Biotechnology Information (NCBI Gene ID 378848). It is very important to make sure to have the correct full-length ORF and note any sequence-specific details like restriction sites or untranslated regions (UTRs). Confirmation of the right ORF was done by translation and comparison with the amino acid sequence from Uniprot reference.

2.3. Extraction of total RNA (tRNA)

Our main objective was to clone the zebrafish BiP ORF, using as original template the totalRNA extracted from Zebrafish. Total RNA was extracted from a caudal zebrafish cell line (SJD:1 from ATCC company) using the E.Z.N.A.® Total RNA Kit I.

The key of the E.Z.N.A.® RNA family of products is that it combines the speed of mini-column spin technology with the reversible binding qualities of the HiBind Matrix, allowing for the processing of one or more samples at once. Phenol/chloroform extractions are less specific, and laborious processes like precipitation with isopropanol or LiCl or CsCl gradient ultracentrifugation are unnecessary.

The Total RNA Kit by E.Z.N.A.® I is capable of purifying up to 100 µg of total RNA from tissue or cultured eukaryotic cells. Typically, a single experiment can process 5–30 mg of tissue or 1×10^6 – 1×10^7 eukaryotic cells. Denaturing circumstances that render RNases inactive cause cells or tissue to lyse. Following the homogenization procedure, samples are placed on the HiBind RNA spin column. After a few fast wash steps, cellular debris and other impurities are successfully removed. Finally, high-quality RNA elutes in water treated with Diethylpyrocarbonate (DEPC)-treated and sterile filtered water, which inactivates RNase enzymes in water by covalent modifications of the histidine residues. This kit is used to isolate total RNA larger than 200 nt.

2.4. Synthesis of cDNA

The NZY first-strand cDNA synthesis kit from NZYtech (MB17001) was used to synthesize the cDNA from total RNA. The NZY First-Strand cDNA Synthesis Kit by NZYtech contains all the components required for the synthesis of first-strand cDNA, except for the template RNA, and the very active NZY Reverse Transcriptase. Random hexamers and Oligo (dT)₁₈ primers are supplied in separate tubes. The NZY First-Strand cDNA Synthesis Kit was designed to boost sensitivity in subsequent applications and yield large amounts of full-length cDNA products. Ten pg to five µg of total RNA can be used as starting material. NZY Reverse Transcriptase (RNase H minus) and a potent NZY Ribonuclease Inhibitor are both included in this mixture to shield RNA from ribonuclease contamination. After the first-strand cDNA synthesis, RNase H (from *E. coli*) is supplied in a different tube to specifically break down the

RNA template in cDNA-RNA hybrids and facilitate PCR primers to anneal to the cDNA in following PCR assays.

To synthesize cDNA, the following components were mixed into autoclaved PCR tubes.

1. 20 μ l of NZYRT 2x master mix
2. 4 μ l NZYRT enzyme mix
3. 4 μ l 400 ng/ μ l RNA
4. 12 μ l DEPC H₂O

We mixed the tubes gently, span down and then incubated at 25 °C for 10 minutes. Then raised the temperature to 50 °C and incubated for 30 minutes. Final heating to 85 °C for 5 minutes, inactivated the reaction. After inactivation, the tubes were chilled on ice, and 1 μ l of NZY RNase was added to each tube and incubated for 20 minutes at 37 °C. The cDNA was stored at – 20 °C.

2.5. PCR to amplify the ORF of zebrafish BiP

The cDNA, non-diluted and diluted 1:10 and 1:100 in autoclaved water, was used as template for the PCR to amplify the ORF of zebrafish BiP. We made positive and control tubes as well. In the positive tubes we poured 32.5 μ l of autoclaved water, 10 μ l 5x reaction buffer, 1 μ l of 10 mM dNTPs, 2.5 μ l of 10 μ M forward primer, 2.5 μ l of 10 μ M reverse primer, 1 μ l of the cDNA template (1, 1:10 and 1:100 dilutions) and 0.5 μ l of supreme DNA polymerase enzyme lastly to avoid non-specific random amplification. For the negative control instead of the template, an extra 1 μ l of autoclaved water was added into the PCR tube.

The following primers were used to amplify ORF of zebrafish BiP using cDNA as template:

FW primer (Bam HI)

5'- ttaggatcc t gtt ggg aca gtg att ggg atc -3'

Rev primer (AflIII/BspTI)

5'- gta cat ctaag cta cag ctc gtc ctt ctc ttc -3'

Adding 4-6 extra nucleotides upstream of restriction sites can enhance enzymatic efficiency.

The PCR cycles were set for the following parameters:

Starting the amplification with HOT START DNA polymerase with a temperature of 96 °C for 4 minutes. Then, 30 cycles were established, each consisting of denaturation at 96 °C for 30 seconds, annealing at three different temperatures (52°C, 55°C, 58°C) for 30 seconds, and

extending at 72°C for 60 seconds. A final step of extension was carried out at 72°C for 10 minutes. After the PCR reaction, 5 µl of 10x green buffer were added and samples were run in an agarose gel 1%.

The preparation of the agarose gel was as follows: 0.5 g agarose powder, 5 ml of TAE Buffer 10x and 45 ml of autoclaved water. The recipe for 1 liter of the 10 x TAE Buffer: 48.5 g tris, 11.4 mL of glacial acetic acid and 20 ml of 0.5 M EDTA (pH 8.0). We heated the agarose mixture in a microwave, until it was boiling, then we cooled it down, and added Green Safe Premium from NZYtech. When GreenSafe stain binds to DNA or RNA, it emitted green fluorescence. It exhibits one strong excitation peak at 490 nm and two secondary fluorescence excitation peaks at about 270 and 290 nm. The samples then were loaded into the agarose gel and the gel ran for 2 hours at 50 VOLT to confirm the PCR product size.

Extracting the amplicon from agarose gel

The amplicon of the right size was extracted from the gel using the kit (NZYGelPure) from NZYtech. The NZYGelPure kit is intended for direct purification of PCR products as well as DNA purification from TAE/TBE agarose gels. DNA fragments ranging in size from 50 bp to 20 kb can be purified using the kit. The NZYGelPure purification kit's silica-gel-based membrane may selectively adsorb up to 20 µg of DNA fragments. Impurities such as soluble agarose, nucleotides, oligos (less than 30 mers), primer dimers, enzymes, mineral oil, and others are washed away because they are unable to attach to the membrane. Following elution from the column, DNA fragments are ready for use in subsequent procedures without additional processing.

Procedure for DNA Purification from Agarose Gels:

All centrifugations should be carried out at room temperature in a table-top micro centrifuge at >12000 x g

1. The DNA fragment from the gel was excised with a clean, sharp scalpel. After weighting the gel slice, it was transferred to a 1.5 mL microcentrifuge tube.
2. 300 µL of Binding Buffer was added for each 100 mg of gel weight.
3. Incubation at 55-60 °C for 5-10 minutes and the tubes were occasionally shake until agarose was completely dissolved.

4. After making sure that the colour of the mixture was yellow, the mixture was loaded into the NZYtech spin column, which was placed into a Collection tube (2 mL). Centrifugation was the next step for 30 s to 1 minute, then flow-through was discarded.
5. 500 μ L of Wash Buffer was added then centrifuged for 30s to 1 minute. Flow-through was discarded.
6. 600 μ L of Wash Buffer was added, then centrifuged for 30s to 1 minute. The flow-through was discarded.
7. To dry NZYtech spin membrane of residual ethanol, centrifugation for 1 minute was essential.
8. The NZYtech spin column was then placed into a clean 1.5 mL microcentrifuge tube. 50 μ L of ultrapure water was added to the centre of the column and incubated at room temperature for 1 minute. The DNA was eluted by centrifugation for 1 minute.
9. Store the purified DNA at -20 °C

2.6 Nested PCR to amplify the ORF of zebrafish BiP

To obtain a significant amount of the ORF of zebrafish BiP and confirm the identity of the band extracted from the PCR that used cDNA as template, a nested PCR was carried out using the band extracted in section 2.5 as template. This product was then diluted 1:10 and 1:100 to be used as a template in the nested PCR.

The PCR cycles were the following:

1. Hot start 96 °C, 4 minutes
 2. Denaturation 96 °C, 30 seconds
 3. Annealing 58 °C, 30 seconds
 4. Extension 72 °C, 60 seconds
 5. Final extension 72 °C, 10 minutes
- 30 cycles from step 2 to 4.

The amplicons with the right size were extracted from the gel as described in section **2.5**.

The constant ϵ is called molar absorptivity or molar extinction coefficient and is a measure of the probability of the electronic transition. For nucleic acids, the absorbance at 260 nm (A_{260}) is used to calculate the concentration, as DNA and RNA absorb UV light strongly at this wavelength due to the presence of nucleotide bases. The measured concentration for the double digested backbone was 12 ng/ μ l.

2.7.2. Double digestion of the PCR product

To create the insert, the PCR product needed to be double digested. We have used the nested PCR product obtained at 58 °C with the template diluted 1:10 (section 2.6).

BspT1 and BamH1 in 2x Tango buffer were used for double digestion, the tubes were gently mixed, spun down, incubated for 16 hours at 37 °C, then inactivated for 20 minutes at 80 °C. Following the double digestion, the PCR product needed to be cleaned with the NZYGELPURE kit, described in section 2.5. Then the concentration of the cleaned PCR product was also measured with NanoDrop One as 23 ng/ μ l.

2.8 Ligation and transformation of *E. coli* DH5 α

2.8.1. Ligation

By using DNA ligase, restriction endonuclease-treated DNA fragments can be covalently recombined. The enzyme synthesizes two phosphodiester bonds using ATP. As soon as we had our backbone and insert double digested, we could carry on and start the ligation. 1 μ l of Speedy ligase from NZYTech, 5 μ l of 4x Speedy Buffer, 3 μ l of the backbone, 10 μ l of the insert and 1 μ l of water was used for the ligation. The whole procedure was prepared on ice. Before using the speedy buffer, since it was very viscous, the buffer needed to be vortexed. The vector and the insert needed to be previously heated at a temperature of 95 °C, for 4 minutes. After adding the buffer, insert the vector into the autoclaved water, the tubes were gently mixed, then spun down. The mixtures were incubated at room temperature for 15 minutes, and then everything was set to perform the transformation.

2.8.2. Transformation

We have used competent DH5 α cells for the transformation, which were stored at -80 °C until use. We added the plasmid to the competent cells, and then chilled the tubes for 20 minutes on ice. Then a step called, “heat shock”, followed this step for 45 seconds, at 42 °C. The tubes then were chilled on ice for another 5 minutes. Afterwards 0.7 ml of LB with no antibiotics was added. The tubes were incubated at 37 °C for 1 hour, and then placed into the centrifuge, to spin down the cells. Some media was removed, and then the cells were re-suspended, and plated on antibiotics containing agar plates, and incubated overnight at 37 °C for the colonies to grow. The next morning the colonies were picked up, grown in liquid media with antibiotic and the NZYMiniprep kit was used to extract the plasmid from the positive ligation mix colonies.

2.9. Minipreps of the construct for zebrafish BiP

The NZYMiniprep kit consists of an alkaline lysis of bacterial cells and DNA adsorption onto silica in the presence of high salt. The silica gel preferentially adsorbed the plasmid DNA while washing away other contaminants, such as proteins, salts, nucleotides, and oligos (less than 40 mers).

For the whole procedure all centrifugations were carried out at room temperature in a table-top microcentrifuge at >12000 g.

The steps to apply the NZYMiniprep kit were the following:

1. Cultivate and harvest bacterial cells

Pellet 1-5 mL of an *E. coli* LB culture with antibiotic for 30 s. Discard the supernatant.

2. Cell Lysis

Re-suspend the cell pellet in 250 μ L Buffer A1 by vigorous vortexing. After this step, we add 250 μ L of Buffer A2 and mixed it. Incubate for 4 minutes at room temperature. Then added 300 μ L Buffer A3.

3. Lysate Clarification

Centrifuge for 5-10 min at room temperature, depending on initial culture volume.

4. DNA Binding

After placing NZYtech spin column in a 2 mL collecting tube, load the supernatant from step 3 onto the column. After centrifugation for 1 min at 11,000 g flow-through was discarded.

5. Wash Silica Membrane

After adding 500 μ L of Buffer AY onto the column, centrifuge it for 1 min, flow-through was discarded.

Then 600 μ L of ethanol containing Buffer A4 was added onto the column, then centrifuged for 1 min, and flow-through was discarded.

6. Dry Silica Membrane

The NZYtech spin column was Re-inserted into the empty 2 mL collecting tube and centrifuged for 2 min.

7. Elute Highly Pure DNA

The dried NZYtech spin column was placed into a clean 1.5 mL microcentrifuge tube and in order to get a higher concentrated miniprep, only 30 μ L of autoclaved water was added into the column. After 1 min of incubation at room temperature, the eppendorf was centrifuged for 1 min. The purified DNA needed to be stored at -20 °C.

Afterwards all the concentrations were measured with NanoDrop One, and the samples were sent to sequencing.

The concentrations were the following:

ZFBip-1 = 64 ng/ μ l

ZFBip-2 = 75 ng/ μ l

ZFBip-3 = 56 ng/ μ l

ZFBip-4 = 44 ng/ μ l

The constructs were sent to STABvida for sequencing using the universal primers:

Universal primers:

Fw pQEPromoter: 5'-CCGAAAAGTGCCACCTG-3'

Rv pQE-R: 5'-GTTCTGAGGTCATTACTGG-3'

2.10. Expression and purification of golden hamster (*Mesocricetus auratus*) BiP (haBiP)

2.10.1 Transformation of *E. coli* BL21 (DE3)

Tubes containing 100 μ L of BL21 (DE3) competent *E. coli* cells prepared as described in section 2.1 were thawed on ice. Then, 1 μ L of plasmid (haBiP_27-654_pQE10, see section 2.2) containing between 1 and 100 ng of DNA was added to the cell suspension, and the tube was kept on ice for 20 minutes. The transformation was performed as mentioned in section 2.8.2. The cells were then incubated at 37 °C for 60 minutes, with shaking at 300 rpm. After the incubation period, the cell suspension was centrifuged at 2300 g at room temperature. 450 μ L of the supernatant was discarded and the cells were resuspended in the remaining 250 μ L, before being plated in plates containing LB agar medium supplemented with 50 μ g.mL⁻¹ of ampicillin and left to incubate overnight at 37°C.

2.10.2 Hamster BiP (haBiP) Expression

A single colony from previously transformed BL21(DE3) competent *E. coli* cells was used to inoculate 50 mL of LB medium containing ampicillin, grown overnight at 37 °C with an agitation of 150 rpm. Large-scale growth cultures were initiated by the addition of 5 mL of the starter culture into 500 mL of LB medium containing ampicillin and were allowed to grow at 37°C until an OD600 of 0.6 to 0.8 was achieved. The expression of haBiP was induced by the addition of IPTG to a final concentration of 500 μ M. The cultures were incubated at 18°C overnight with 100 rpm agitation. The cells were then centrifuged at 6000 g at a temperature

of 4°C, resuspended in HK buffer (50 mM HEPES, 75 mM KCl, pH = 7.4) with 40 mM Imidazole and stored at -20°C.

2.10.3 Hamster BiP Purification

Resuspended cells were thawed on ice and lysed by sonication with an amplitude of 60%, a pulse of 15 seconds on and 20 seconds off, in the presence of DNase, RNase, and proteases inhibitors. The lysed cells were then centrifuged at 12,000 g at 4°C for one hour. The supernatant was collected and filtered using a 0.45 µm filter before being loaded onto a 5 mL HisTrap HP column (Cytiva). The flow-through was collected with 50 mL of buffer HK with 40 mM Imidazole (pH = 7.4). The protein was then eluted by a gradient from HK buffer with 40 mM imidazole to HK with 500 mM imidazole over a volume of 50 mL. The eluted protein was then dialyzed against HK buffer (pH = 7.4) using a Snakeskin membrane (ThermoFisher) with a molecular weight cutoff of 10000 Da. The concentration of BiP was assessed through nanodrop (ϵ at 280 nm for BiP is 29005 M⁻¹cm⁻¹) reaching a concentration of 257 µM, and the purity of the eluted protein was evaluated by a 12% sodium dodecyl sulphate polyacrylamide gel electrophoresis (SDS-Page).

SDS-Page

The gel was prepared as described in the table below:

Table 1. Volumes of the different reagents used to prepare an SDS-Page

	Stacking 4 % (mL)	Resolving 12% (mL)
40 % Acrylamide/Bis	0.69	7.5
Solution 29:1		
0.5 M Tris-HCl pH 6.8 + 0.4% SDS	0.68	-
1.5 M Tris-HCl pH 8.8 +0.4 % SDS	-	6.25
Water	4.44	11.15
10 % APS	0.025	0.1
TEMED	0.005	0.01
Total	6.8	25

3. Results and Discussion

3.1. Cloning the ORF of zebrafish BiP

3.1.1. PCR to amplify the ORF of zebrafish BiP

The cDNA was synthesized from total RNA as described in section 2.4. The ORF of zebrafish BiP was obtained at NCBI (gene ID 378848 and NCBI Reference Sequence: NM_213058.1):

```
1 at gcggttgctt tgctgtttt tgctggggc cggcagcgtg
43 ttgccaag aggacgataa gaaggagagt gttgggacag tgattgggat cgacctcggg
103 accacatact cctgtgttg agtctacaag aatggccgtg ttgagattat tgccaatgac
163 caggaaacc gcatcactcc gtcatacgtg gcctttacca ctgaaggaga gcggtcatc
223 ggagatgctg cgaagaacca gtcacatcc aacctgaaa aactgtgtt tgacgccaag
283 aggctgatcg gacgcacatg gggcgactct tctgtgcagc aggacatcaa atactcccc
343 ttaaggtga tcgagaagaa aaacaagcct cacatccagc tggacatcgg ctctggtcag
403 atgaagacgt ttgaccgga ggaaattcc gccatggtt tgaccaagat gaaggaaacc
463 gcagaggctt atctgggaaa gaaggtcact catgctgtgg tcaccgttcc tgctatttc
523 aacgatgctc agcgtcaggc cactaaagat gctggaacca ttgctgggct gaatgtcatg
583 aggatcatca atgagcctac ggcggctgcc atgcatacg gtctggacaa gagggacgga
643 gagaaaaaca tctgtgtgtt cgatctgggt ggtggcacct ttgacgtgtc tctgtgacc
703 atcgataacg gcgtgttga agtggggcc acaaacggag aactcacct ggcggagaa
763 gacttcgacc agcgcgtcat ggagcacttc atcaagctgt acaagaagaa gacgggcaaa
823 gacgtgcgca aagacaaccg cgccgtgcag aagctgcgca gagaggtgga gaaggctaag
883 agagcgtgt ctgcccagca tcaggcccgc atcgagatcg agtccttctt tgaaggagaa
943 gatttctctg agactctcac cagagccaag ttgaggagc tcaacatgga ctgttccgc
1003 tccactatga agccggttca gaaggttctg gaggactctg acccgaagaa gccagatata
1063 gatgagatcg tgctggtcgg cggctccact cgtatcccga agatccagca gctggtgaag
1123 gagttcttca acgaaaaga gccgtccaga ggaatcaacc ctgacgaggc cgtggcgtac
1183 ggagctgctg tccaggctgg agtctgtcc ggagaggagg agaccggtga tctggttctt
1243 ctggacgtgt gtccgtgac tctgggcatt gagactgtg gaggagtgat gaccaaactc
1303 attcccagaa aactgttgt tcccaccaag aaatcccaga tcttccac tgcttccgac
1363 aaccagccca ccgtcactat caaagttat gagggcgagc gtcccctgac caaagacaac
```

1423 catctgctgg gcacctttga cctgacaggc atccctccag cacctcgtgg tgtcccacag
1483 atcgaggtaa ctttcgagat cgacgtcaac ggcacccctgc gcgtcaccgc cgaagacaaa
1543 ggcaccggaa acaaaaacaa gatcaccatt accaacgacc agaaccggct gaccctgag
1603 gacatcgaga gaatggtgaa cgaagccgag agattcgtg atgaggacaa gaaactgaag
1663 gagagaatcg acagccgcaa tgaattggag agctacgcct attccctgaa gaaccagatc
1723 ggggataaag agaaattagg cggaaagtta tcctctgaag acaaggaggc catcgagaag
1783 gcagtggagg agaagatcga gtggctggag gcgcatcagg acgccgatct ggaggaattc
1843 caggccaaaa agaaggagct ggaggaggtg gtgcagccca tcgtcagcaa actgtacggc
1903 agtgcgggag gaccaccgcc tgaagaggcc gaagagaagg acgagctgta g

The first 16 codons (48 nucleotides) code for a peptide signal that directs the newly synthesized protein to the endoplasmic reticulum (also called secretory pathway) and therefore are useless to express the protein in *E coli*, which has no secretory pathway. The next 8 codons (24 nucleotides) code for a highly charged sequence (GluGluAspAspLysLysGluSer) that was not included as part of the golden hamster BiP previously cloned in pQE10 vector to be expressed in *E coli* (a kind gift from David Ron, University of Cambridge). Therefore, since we want to compare the zebrafish BiP with mammalian BiP from golden hamster to analyse how BiP has evolved in its chaperone function, we have decided to start the amplification at the codons gtt ggg aca..... coding for the residues ValGlyThr.

The PCR to amplify the ORF of zebrafish BiP starting on Val25 was carried out using the appropriate primers (see section 2.5) and cDNA diluted 1:10 and 1:100 as a template. An agarose gel was run to check the size of the bands (Figure 3.1).

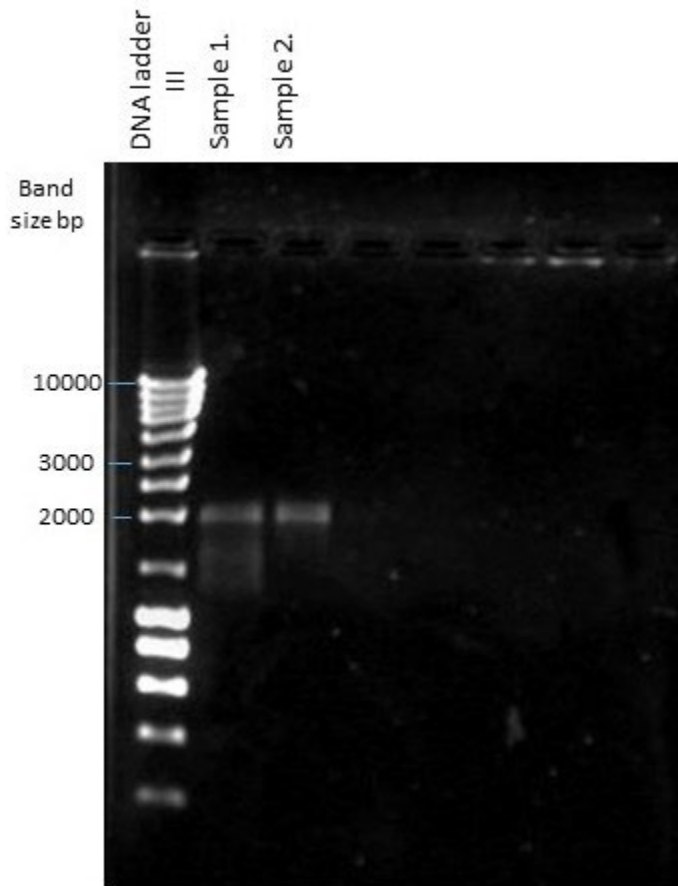


Figure 3.1 Agarose gel (1%) showing the amplicons from the PCR using cDNA as template using . Sample 1 is the dilution of 1:10 of the cDNA used as template, Sample 2 is the dilution of 1:100 of the cDNA used as template We were expecting a band with a size of 1881 bp.

An amplicon of 1881 bp is expected after discounting the first 72 nucleotides from the ORF of zebrafish shown above and indeed a band of around 2000 bp was observed in the gel indicating that amplification was successful.

3.1.2. Nested PCR to amplify the ORF of zebrafish BiP

To obtain a significant amount of the ORF of zebrafish BiP and confirm the identity of the band extracted from the PCR that used cDNA as template, a nested PCR was carried out using the bands extracted from the gel shown in figure 3.1 The gel in Figure 3.2 shows the amplicons from the nested PCR with a strong band around 2000 bp as expected. To get a more concentrated insert, the nested PCR reaction was repeated using as template the band extracted from the gel after dilution 1:100.

The amplicons with the right size were extracted from the gel and sent to sequencing to confirm the identity of the amplicon.

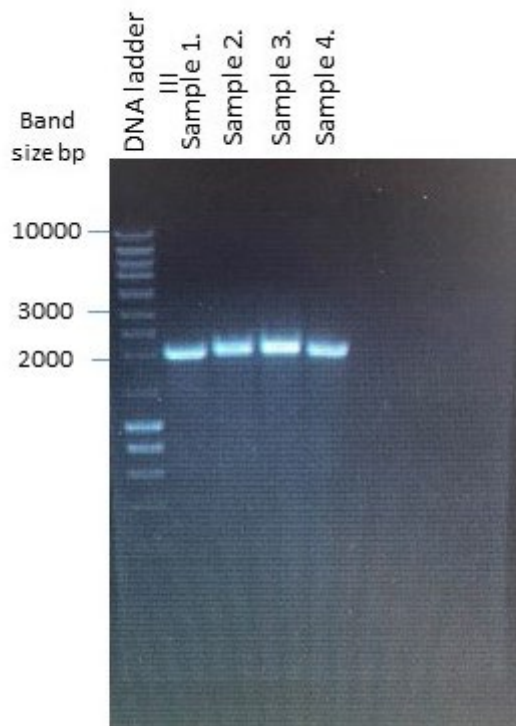


Figure 3.2 Nested PCR product where Sample1, Sample 2 are PCR products using cDNA template diluted 1:10; Sample 3, Sample 4 are PCR products using cDNA template diluted 1:100.

The sequence of the PCR product obtained with the forward primer used for amplification is compared with the expected zebrafish ORF from Val 25:

Alignment of Sequence_1: [ORF zebrafish from Val25.xdna] with Sequence_2: [PCR product FW.xdna]

Similarity: 1104/1107 (99.73 %)

Seq_1 1 Gttgggacagtgattgggatcgacctcgggaccacatactcctgtgttgagctctacaag 60

|||||

Seq_2 1 -----TTGGAGTCTACAAG 14

Seq_1 61 aatggccgtgttgagattattgccaatgaccagggaaccgcatcactccgtcatacgtg 120

|||||

Seq_2 15 AATGGCCGTGTTGAGATTATTGCCAATGACCAGGGAACCGCATCACTCCGTCATACGTA 74

Seq_1 121 gcctttaccactgaaggagagcggctcatcggagatgctgcaagaaccagctcacatcc 180
 |||
 Seq_2 75 GCCTTTACCACTGAAGGAGAGCGGCTCATCGGAGATGCTGCGAAGAACCAGCTCACATCC 134

Seq_1 181 aaccctgaaaacactgtggttgacgccaagaggctgatcggacgcacatggggcgactct 240
 |||
 Seq_2 135 AACCTGAAAACACTGTGTTTGACGCCAAGAGGCTGATCGGACGCACATGGGGCGACTCT 194

Seq_1 241 tctgtgcagcaggacatcaaatacttccccttaagtgatcgagaagaaaaacaagcct 300
 |||
 Seq_2 195 TCTGTGCAGCAGGACATCAAATACTTCCCCTTAAGGTGATCGAGAAGAAAAACAAGCCT 254

Seq_1 301 cacatccagctggacatcggctctggtcagatgaagacgtttgcaccggaggaaattcc 360
 |||
 Seq_2 255 CACATCCAGCTGGACATCGGCTCTGGTCAGATGAAGACGTTTGCACCGGAGGAAATTCC 314

Seq_1 361 gccatggttttgaccaagatgaaggaaccgcagaggcttatctgggaaagaaggtcact 420
 |||
 Seq_2 315 GCCATGGTTTTGACCAAGATGAAGGAAACCGCAGAGGCTTACTTGGGAAAGAAGGTCACT 374

Seq_1 421 catgctgtggtcaccgttcctgcttatttcaacgatgctcagcgtcaggccactaaagat 480
 |||
 Seq_2 375 CATGCTGTGGTCACCGTTCCTGCTTATTTCAACGATGCTCAGCGTCAGGCCACTAAAGAT 434

Seq_1 481 gctggaaccattgctgggctgaatgtcatgaggatcatcaatgagcctacggcggtgcc 540
 |||
 Seq_2 435 GCTGGAACCATTGCTGGGCTGAATGTCATGAGGATCATCAATGAGCCTACGGCGGTGCC 494

Seq_1 541 attgcatacgtctgacaagaggacggagagaaaaacatcctggtgttcgatctgggt 600
 |||
 Seq_2 495 ATCGCATACGGTCTGGACAAGAGGGACGGAGAGAAAAACATCCTGGTGTTCGATCTGGGT 554

Seq_1 601 ggtggcacctttgacgtgtctctgctgaccatcgataacggcgtggttgaagtgggtgcc 660
 |||
 Seq_2 555 GGTGGCACCTTTGACGTGTCTCTGCTGACCATCGATAACGGCGTGTGGAAGTGGTGGCC 614

Seq_1 661 acaaacggagacactcacctgggCGGAGAAGACTTCGACCAGCGTCATGGAGCACTTC 720
 |||

Seq_2 615 ACAAACGGAGACTCACCTGGGCGGAGAAGACTTCGACCAGCGTCATGGAGCACTTC 674

Seq_1 721 atcaagctgtacaagaagaagacgggcaaagacgtgCGCAAAGACAACCGCGCCGTGCAG 780
 |||

Seq_2 675 ATCAAGCTGTACAAGAAGAAGACGGGCAAAGACGTGCGCAAAGACAACCGCGCCGTGCAG 734

Seq_1 781 aagctgCGCAGAGAGGTGGAGAAGGCTAAGAGAGCGTGTCTGCCAGCATCAGGCCGC 840
 |||

Seq_2 735 AAGCTGCGCAGAGAGGTGGAGAAGGCTAAGAGAGCGTGTCTGCCAGCATCAGGCCGC 794

Seq_1 841 atcgagatcgagtccttcttgaaggagaagatttctctgagactctcaccagagccaag 900
 |||

Seq_2 795 ATCGAGATCGAGTCCTTCTTTCAGGGAGAAGATTCTCTGAGACTCTCACCAGAGCCAAG 854

Seq_1 901 tttgaggagctcaacatggacttggtccgctccactatgaagccggttcagaaggttctg 960
 |||

Seq_2 855 TTTGAGGAGCTCAACATGGACTTGTCCGCTCCACTATGAAGCCGGTTCAGAAGGTCTCG 914

Seq_1 961 gaggactctgacccgaagaagccagatcctgatgagatcgtgctggtcgCGGCTCCACT 1020
 |||

Seq_2 915 GAGGACTCTGACCTGAAGAAGCCAGATATTGATGAGATCGTGTGGTTCGGCGGCTCCACT 974

Seq_1 1021 cgtatcccgaagatccagcagctggtgaaggagtcttcaacggaaaagagccgtccaga 1080
 |||

Seq_2 975 CGTATCCCGAAGATCCAGCAGCTGGTGAAGGAGTTCTTCAATGGAAAAGAGCCGTCCAGA 1034

Seq_1 1081 ggaatcaaccctgacgagggcCGTGGGTACGGAGCTGCTGTCCAGGCTGGAGTCTGTCC 1140
 |||

Seq_2 1035 GGAATCAACCCTGACGAGGCCGTGGCGTACGGAGCTGCTGTCCAGGCTGGAGTCTGTCC 1094

Seq_1 1141 ggagaggaggagaccggtgatctggttcttctggacgtggtccgctgactctggcatt 1200
 |||

Seq_2 1095 GGA----- 1097

There are 5 silent mutations (see codons in green) but there is one missense mutation from a Proline to a Leucine (see codon in red). The sequence was checked until nucleotide 1095 (see PDF file with the chromatogram in annex B), so translation was checked from residue 41 to 381 in 627.

Below is the comparison between zebrafish ORF from Val 25 and PCR product sequenced from reverse primer (reverse complementary sequence from nucleotide sequence):

Alignment of Sequence_1: [ORF zebrafish from Val25.xdna] with Sequence_2: [PCR product Rv-rev-comp.xdna]

Similarity: 1146/1148 (99.83 %)

```

Seq_1  661  acaaacggagacactcacctggcgagaagacttcgaccagcgcgtcatggagcacttc  720
      ||||||||||||||||||
Seq_2  2      -----GTCATGGAGCACTTC  16

Seq_1  721  atcaagctgtacaagaagaagacgggcaaagacgtgcgcaaagacaaccgcccgtgcag  780
      ||||||| |||||||||||||||||||||||||||||||||||||||||||||||
Seq_2  17  ATCAAGCTTTACAAGAAGAAGACGGGCAAAGACGTGCGCAAAGACAACCGCCCGTGCAG  76

Seq_1  781  aagctgcgagagaggtggagaaggctaagagagcgtgtctgcccagcatcaggcccgc  840
      ||||||||||||||| |||||||||||||||||||||||||||||||||||||||
Seq_2  77  AAGCTGCGCAGAGAG-TGGAGAAGGCTAAGAGAGCGCTGTCTGCCCAGCATCAGGCCGC  135

Seq_1  841  atcgagatcgagtccttctttgaaggagaagatttctctgagactctcaccagagccaag  900
      ||||||||||||||| |||||||||||||||||||||||||||||||||||||||
Seq_2  136  ATCGAGATCGAGTCCTTCTTTGAGGGAGAAGATTTCTCTGAGACTCTCACCAGAGCCAAG  195

Seq_1  901  tttgaggagctcaacatggacttggtccgctccactatgaagccggttcagaaggttctg  960
      ||||||||||||||| |||||||||||||||||||||||||||||||||||||||
Seq_2  196  TTTGAGGAGCTCAACATGGACTTGTTCCGCTCCACTATGAAGCCGGTTCAGAAGTTCTG  255

Seq_1  961  gaggactctgaccggaagaagccagatatcgatgagatcgtgctggcggcgtccact  1020
      ||||||||||||||| |||||||||||||||||||||||||||||||||||||||
Seq_2  256  GAGGACTCTGACCTGAAGAAGCCAGATATTGATGAGATCGTGTGGTCGGCGGCTCCACT  315

```

Seq_1 1021 cgtatcccgaagatccagcagctggtgaaggagtctttc**aac**ggaaaagagccgtccaga 1080
 |||
 Seq_2 316 CGTATCCCGAAGATCCAGCAGCTGGTGAAGGAGTTCTTC**AAT**GGAAAAGAGCCGTCCAGA 375

Seq_1 1081 ggaatcaaccctgacgagggcctggcgtaacgagctgctgtccaggetggagtctgtcc 1140
 |||
 Seq_2 376 GGAATCAACCCTGACGAGGCCGTGGCGTACGGAGCTGCTGTCCAGGCTGGAGTCCTGTCC 435

Seq_1 1141 ggagaggaggagaccggtgatctggttctcttgacgtgtgtccgctgactctgggcatt 1200
 |||
 Seq_2 436 GGAGAGGAGGAGACCGGTGATCTGGTTCTTCTGGACGTGTGTCCGCTGACTCTGGGCATT 495

Seq_1 1201 gagactgttgaggagtgatgaccaaactcattcccagaaactgttgttcccaccaag 1260
 |||
 Seq_2 496 GAGACTGTTGGAGGAGTGATGACCAAACCTCATTTCCAGAAACTGTTGTTCCACCAAG 555

Seq_1 1261 aaatcccagatctttctccactgcttccgacaaccagcccaccgtcactatcaagtttat 1320
 |||
 Seq_2 556 AAATCCCAGATCTTCTCCACTGCTTCCGACAACCAGCCCACCGTCACTATCAAAGTTTAT 615

Seq_1 1321 gagggcgagcgtcccctgaccaaagacaacatctgctgggcacctttgacctg**aca**ggc 1380
 |||
 Seq_2 616 GAGGGCGAGCGTCCCCTGACCAAAGACAACCATCTGCTGGGCACCTTTGACCTG**ACT**GGC 675

Seq_1 1381 atccctccagcacctcgt**ggt**gtcccacagatcgaggtaactttcgagatcgacgtcaac 1440
 |||
 Seq_2 676 ATCCCTCCAGCACCTCGT**GGC**GTCACAGATCGAGGTAACTTTCGAGATCGACGTCAAC 735

Seq_1 1441 ggcacctgcgcgtcaccgccgaagacaaaggcaccggaaacaaaaacaagatcaccatt 1500
 |||
 Seq_2 736 GGCATCCTGCGCGTCAACGCCGAAGACAAAGGCACCGGAAACAAAAACAAGATCACCATT 795

Seq_1 1501 accaacgaccagaaccggctgaccctgaggacatcgagagaatggtgaacgaagccgag 1560
 |||
 Seq_2 796 ACCAACGACCAGAACCGGCTGACCCCTGAGGACATCGAGAGAATGGTGAACGAAGCCGAG 855

```

Seq_1 1561 agattcgctgatgaggacaagaaactgaaggagagaatcgacagccgcaatgaattggag 1620
      |||
Seq_2 856 AGATTTCGCTGATGAGGACAAGAAACTGAAGGAGAGAATCGACAGCCGCAATGAATTGGAG 915

Seq_1 1621 agctacgcctattccctgaagaaccagatcggggataaagagaaattaaggcggaaagtta 1680
      |||
Seq_2 916 AGCTACGCCTATTCCCTGAAGAACCAGATCGGGGATAAAGAGAAATTAAGTGGAAAGTTA 975

Seq_1 1681 tcctctgaagacaaggaggccatcgagaaggcagtgaggagagaagatcgagtggctggag 1740
      |||
Seq_2 976 TCCTCTGAAGACAAGGAGGCCATCGAGAAGGCAGTGGAGGAGAAGATCGAGTGGCTGGAG 1035

Seq_1 1741 gcgcatcaggacgccgatctggaggaattccaggccaaaagaaggagctggaggaggtg 1800
      |||
Seq_2 1036 GCGCATCAGGACGCCGATCTGGAGGAATTCAGGCCAAAAGAAGGAGCTGGAGGAGGTG 1095

Seq_1 1801 gtgcagcccatcgctcagcaaaactgtacggcagtgcgggaggaccaccgcctgaagaggcc 1860
      |||
Seq_2 1096 GTGCAGCCCATCGCTCAGCAAACCTGTACGGCAGTGCGGGAGGACCACCGCC----- 1145

Seq_1 1861 gaagagaaggacgagctgtag 1881

Seq_2 1146 ----- 1145

```

There are 9 silent mutations (see codons in green) and the same missense mutation from a Proline to a Leucine at position 374 (see codon in red) found in the forward sequencing. The G deletion in nucleotide 92 of the reverse sequence was observed in the chromatogram as a shoulder. The sequence of the PCR product was checked from nucleotide 705 until nucleotide 1849 based on the reverse sequence (see PDF with the chromatogram), so translation was checked from residue 235 to 616.

Joining the information from the forward and reverse sequence, the PCR product was checked from residues 41 to 616 in 627 residues for the full length protein. The beginning and the end of the sequence of the PCR product could not be verified because we used the same primers used in the PCR reaction. Anyway, 92% of the sequence of the PCR product was checked and

only the missense mutation from Pro to Leu at position 334 was found. This is a very strong indication that we have succeeded in the amplification of the ORF of zebrafish BiP.

3.1.2 Backbone

The backbone (haBiP_27-654_pQE10, see Material and Methods, section 2.2) and the ORF of zebrafish BiP used as insert were double digested with BamHI and Bspt1 restriction enzymes as described in section 2.7

To test the restriction enzymes and respective buffers, four single digestions and one double digestion were performed (Figure 3.3).

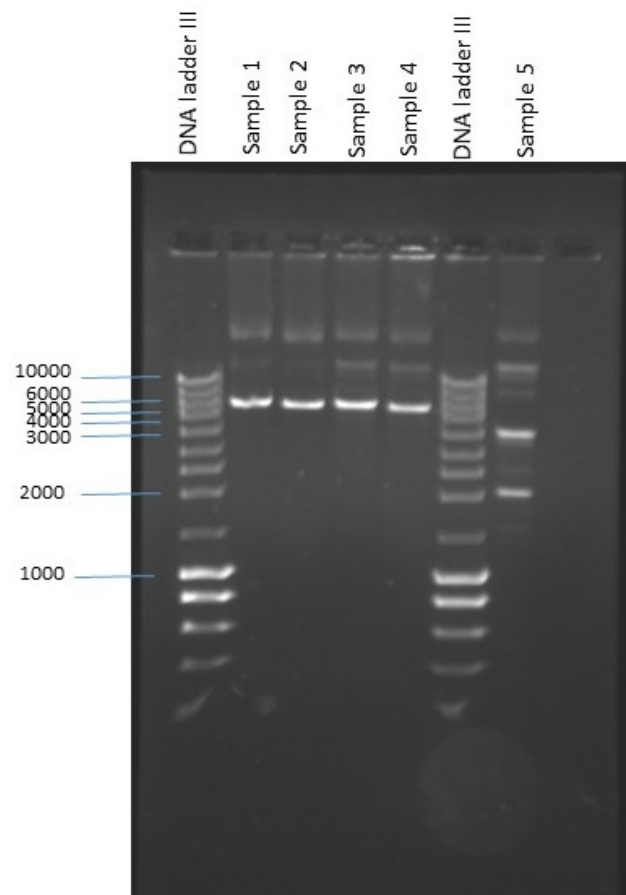


Figure 3.3 Four single, and one double digestion of the pQE10 vector to be used as backbone. Sample 1. Bspt1+ Buffer Tango ; Sample 2. Bspt1+ Buffer O; Sample 3. BamH1+Buffer Tango; Sample 4. BamH1+ Buffer BamH1+; Sample 5. Bspt1 + BamH1 + Buffer Tango. The

size of single digested band shown in samples 1, 2, 3 and 4 is 5749 bp, for sample 5, which is the double digested vector, the size of the first band is 3779 and band two is 1970 bp.

After testing the restriction endonucleases and the respective buffers, the haBiP_27-654_pQE10 vector was double digested with BamH1 and Bspt1 using buffer Tango to remove haBiP. The results are shown in Figure 3.4

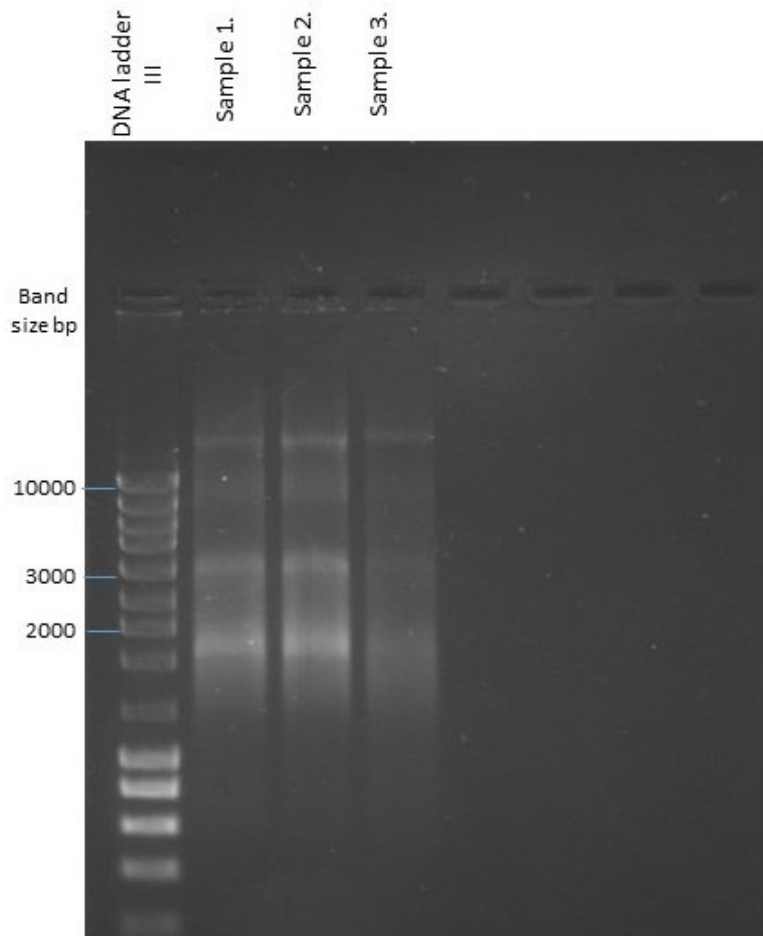


Figure 3.4 Double digested backbone with the restriction enzymes BamH1 and Bspt1 in buffer Tango. Sample 1., Sample 2 and Sample 3 are replicates. As referred in figure 3.3, expected sizes after double digestion are 3779 bp for the backbone and 1970 bp for the insert to be removed.

3.1.3 Ligation and Transformation

The ligation of the ORF of zebrafish BiP after double digestion into the backbone pQE10 after removing hamster BiP was carried out using a ratio insert: backbone 10:1 (v/v). To allow us to identify background colonies that arise from self-ligated backbone, a negative control without insert was carried out. After transformation of competent cells with the ligation mixture and the negative control that contains only the backbone, the cells were plated on agar plates with ampicillin.

Ideally, the negative control should have very few or no colonies, indicating minimal background from the backbone. There were a few colonies in the plates with the full ligation mixture, and minipreps from those colonies were prepared and sent to sequencing using the universal forward primer pQEPromoter as described in section 2.9. Below is a comparison of one miniprep sequence with the sequence expected for the ORF of zebrafish BiP.

from Val 25). As the sequence of the PCR product was verified to be the right sequence (see section 3.1.2), we can conclude that *E coli* cells have recombined the ORF of zebrafish BiP after transformation. This result was unexpected, but *E coli* can indeed recombine certain DNA sequences (Persky & Lovett, 2008).

3.2.Expression and Purification of hamster BiP

3.2.1. IMAC Purification (Immobilized Metal Affinity Chromatography)

The ORF of hamster BiP cloned into vector haBiP_27-654_pQE10 was expressed in LB medium with ampicillin overnight at 18 °C as described in material and methods (section 2.10). Hamster BiP in this vector contains a polyhistidine tag (His-tag) with six histidine residues at the N-terminal. IMAC is a chromatographic method used to purify proteins containing an His-tag. The resin used for IMAC contains immobilized metal ions, such as Ni²⁺ (nickel), which bind specifically to the histidine residues in the His-tagged proteins. The chromatogram for the purification of hamster BiP is shown in Figure 3.5.

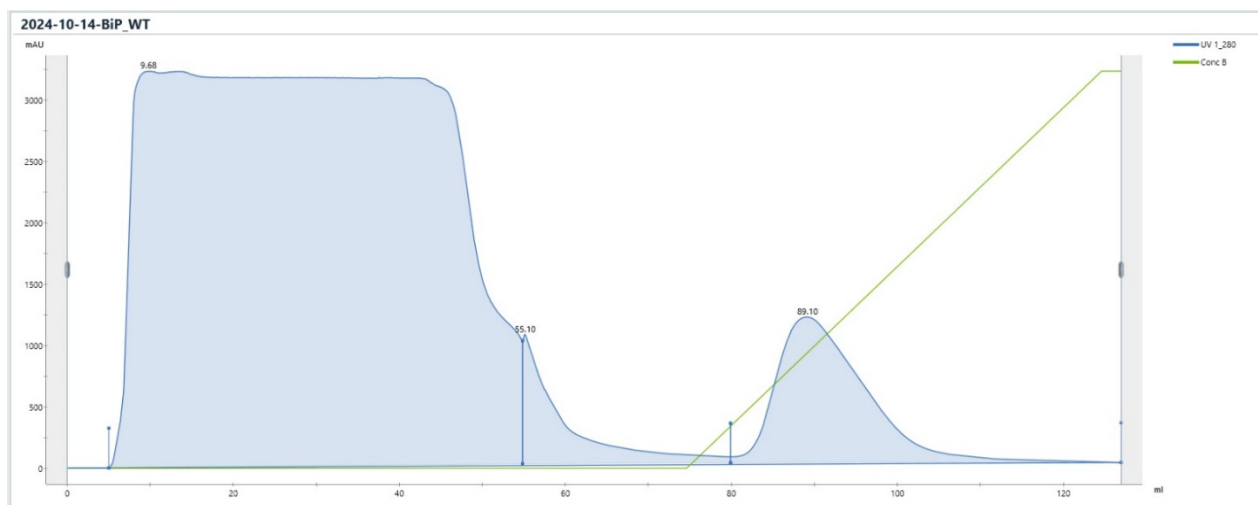


Figure 3.5 Chromatogram for the purification of golden hamster BiP showing (starting at 9.68 mL) the flow-through, which is the first large peak at the beginning of the run and the elution peak corresponding (at 89.10 mL) to the elution of BiP under increasing imidazole concentration.

The flow-through (starting at 9.68 mL) is expected to contain all the proteins from *E. coli* that do not bind to the nickel ions on the column because they do not have an His-tag. The elution peak (peak at 89.10 mL) should correspond to the BiP protein eluted during the gradient that increases the concentration of imidazole (green line in figure 3.5) which competes with the His-tag for the binding to the nickel ions in the column.

To remove the Imidazole, the eluted fractions containing Bip were subjected to dialysis against TR Buffer (50mM Tris-HCl, 200 mM NaCl) overnight using a SnakeSkin dialysis membrane (Thermofisher) with a cutoff of 10,000 Da.

3.2.2. SDS page

The purity of the eluted BiP was analyzed by a 12% SDS-PAGE (Figure 3.6)

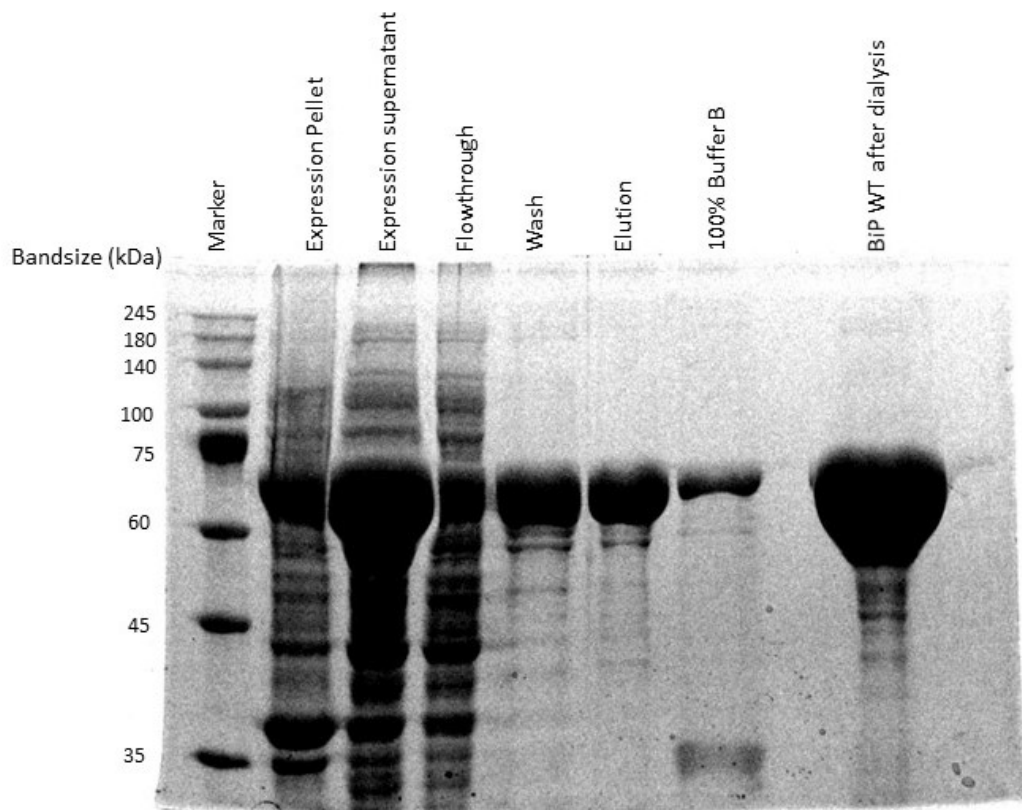


Figure 3.6 SDS Page showing the different fractions from the purification of hamster BiP by IMAC.

The molecular weight of hamster BiP is 71043 Da and the extinction coefficient at 280 nm is $29005 \text{ M}^{-1}\text{cm}^{-1}$ as calculated by ProtParam from Expasy (<https://web.expasy.org/cgi-bin/protparam/protparam>). A fraction of BiP is insoluble when expressed in *E. coli* as revealed by the strong band at the right size in the lane identified as expression pellet. However, a major fraction is soluble in the supernatant after cell disruption, lane expression supernatant. In the flowthrough, proteins that have no affinity or very little affinity to the nickel ion can be found. Based on the analysis of the wash fraction, the column should be saturated and some weakly bound BiP was washed away previously to the elution gradient. BiP was eluted during the gradient to 500 mM imidazole (lane elution). At 500 mM imidazole (100% buffer B after the gradient) there is still a bit of BiP eluted from the nickel along with a faint band of a significantly smaller protein, which might be a truncated version of BiP based on the strong affinity to nickel ions. After dialysis to remove imidazole, the fraction of eluted BiP was concentrated to around 120 μM (measured based on the extinction coefficient at 280 nm) and analyzed on the gel to reveal a degree of purity over 95% (lane BiP WT after dialysis).

Conclusions

With an expected amplicon size of 1881 bp, the study successfully amplified the BiP ORF from zebrafish using reverse transcriptase and PCR, as validated by nested PCR. 99.73% similarity with the predicted zebrafish ORF was confirmed by sequencing the PCR product, which revealed one missense mutation (proline to leucine at location 334). After the golden hamster BiP sequence was removed, the pQE10 vector was used as the backbone. The backbone preparation was prepared by double digestion with BamHI and BsptI, and the zebrafish BiP ORF was ligated into the vector with a 10:1 insert-to-backbone ratio. Colony screening after transformation into *E. coli* DH5 α showed some background from the self-ligated backbone, but minipreps from colonies in the positive plates were sent for sequencing. The zebrafish BiP sequence was recombined by *E. coli*, indicating the necessity of using a recombination-deficient *E. coli* strain for successfully cloning the ORF of zebrafish BiP.

Additionally, golden hamster BiP was successfully expressed in *E. coli* BL21 (DE3) and purified by Immobilized Metal Affinity Chromatography (IMAC). A distinct elution peak in

the chromatogram analyzed by SDS-page showed that the His-tagged BiP had effectively bound to the Ni²⁺ column and was eluted by imidazole with a purity degree over 95%.

These results lay the groundwork for comparing the roles of BiP in zebrafish and mammals, namely in the areas of protein disaggregation and chaperone-mediated neuroprotection. Research on the evolutionary adaptations of BiP in vertebrates will be possible if the recombination in *E. coli* is solved.

In the future, we may be able to find novel strategies to treat proteostasis imbalances by comprehending how BiP interacts with co-chaperones and substrates. Modifying BiP activity may help treat disorders brought on by protein aggregation, which has potential implications for drug discovery. To compare with mammalian orthologs and investigate the precise biochemical and cellular pathways regulated by zebrafish BiP, more research is necessary. This study provides a solid basis for expanding our knowledge of chaperone biology and devising new approaches to treat neurodegenerative diseases.

References

- Aliyu, H., Habibu, Anke Neumann, A., & Ochsenreither, K. (2024). Enzymes in molecular biotechnology. In K.-E. Jaeger (Ed.), *Introduction to enzyme technology* (pp. 431–467). Springer International Publishing. https://doi.org/10.1007/978-3-031-42999-6_20
- Anttonen, A. K., Mahjneh, I., Hämäläinen, R. H., Lagier-Tourenne, C., Kopra, O., Waris, L., Anttonen, M., Joensuu, T., Kalimo, H., Paetau, A., Tranebjaerg, L., Chaigne, D., Koenig, M., Eeg-Olofsson, O., Udd, B., Somer, M., Somer, H., & Lehesjoki, A. E. (2005). The gene disrupted in Marinesco-Sjögren syndrome encodes SIL1, an HSPA5 cochaperone. *Nature Genetics*, 37(12), 1309–1311. <https://doi.org/10.1038/ng1677>
- Assenza, S., Sassi, A. S., Kellner, R., Schuler, B., De Los Rios, P., & Barducci, A. (2019). Efficient conversion of chemical energy into mechanical work by Hsp70 chaperones. *eLife*, 8, e48491. <https://doi.org/10.7554/eLife.48491>
- Bedows, E. D. (1977). Studies on prokaryotic and eukaryotic polynucleotide ligases (Publication No. 2142/68078) [Doctoral dissertation, University of Illinois at Urbana-Champaign]. Illinois Digital Environment for Access to Learning and Scholarship (IDEALS). <http://hdl.handle.net/2142/68078>
- Beissinger, M., & Buchner, J. (1998). How chaperones fold proteins. *Biological Chemistry*, 379(3), 245–259. <https://doi.org/10.1515/BC.1998.033>
- Bertelsen, E. B., Chang, L., Gestwicki, J. E., & Zuiderweg, E. R. (2009). Solution conformation of wild-type E. coli Hsp70 (DnaK) chaperone complexed with ADP and substrate. *Proceedings of the National Academy of Sciences of the United States of America*, 106(21), 8471–8476. <https://doi.org/10.1073/pnas.0903503106>
- Blond-Elguindi, S., Cwirla, S. E., Dower, W. J., Lipshutz, R. J., Sprang, S. R., Sambrook, J. F., & Gething, M. J. (1993). Affinity panning of a library of peptides displayed on bacteriophages reveals the binding specificity of BiP. *Cell*, 75(4), 717–728. [https://doi.org/10.1016/0092-8674\(93\)90492-9](https://doi.org/10.1016/0092-8674(93)90492-9)
- Blond-Elguindi, S., Fourie, A. M., Sambrook, J. F., & Gething, M. J. (1993). Peptide-dependent stimulation of the ATPase activity of the molecular chaperone BiP is the result of conversion of oligomers to active monomers. *Journal of Biological Chemistry*, 268(17), 12730–12735. [https://doi.org/10.1016/S0021-9258\(18\)31449-2](https://doi.org/10.1016/S0021-9258(18)31449-2)

Booth, L., Roberts, J. L., Cash, D. R., Tavallai, S., Jean, S., Fidanza, A., Cruz-Luna, T., Siembiba, P., Cycon, K. A., Cornelissen, C. N., & Dent, P. (2015a). GRP78/BiP/HSPA5/DnaK is a universal therapeutic target for human disease. *Journal of Cellular Physiology*, 230(7), 1661–1676. <https://doi.org/10.1002/jcp.24919>

Booth, L., Roberts, J. L., & Dent, P. (2015b). HSPA5/DnaK may be a useful target for human disease therapies. *DNA and Cell Biology*, 34(3), 153–158. <https://doi.org/10.1089/dna.2015.2808>

Bracher, A., & Verghese, J. (2015). The nucleotide exchange factors of Hsp70 molecular chaperones. *Frontiers in Molecular Biosciences*, 2, 10. <https://doi.org/10.3389/fmolb.2015.00010>

Buchberger, A., Theyssen, H., Schröder, H., McCarty, J. S., Virgallita, G., Milkereit, P., Reinstein, J., & Bukau, B. (1995). Nucleotide-induced conformational changes in the ATPase and substrate binding domains of the DnaK chaperone provide evidence for interdomain communication. *Journal of Biological Chemistry*, 270(28), 16903–16910. <https://doi.org/10.1074/jbc.270.28.16903>

Campion, D., Pottier, C., Nicolas, G., Le Guennec, K., & Rovelet-Lecrux, A. (2016). Alzheimer disease: Modeling an A β -centered biological network. *Molecular Psychiatry*, 21(7), 861–871. <https://doi.org/10.1038/mp.2016.38>

Campion, D., Dumanchin, C., Hannequin, D., Dubois, B., Belliard, S., Puel, M., Thomas-Anterion, C., Michon, A., Martin, C., Charbonnier, F., Raux, G., Camuzat, A., Penet, C., Mesnage, V., Martinez, M., Clerget-Darpoux, F., Brice, A., & Frebourg, T. (1999). Early-onset autosomal dominant Alzheimer disease: Prevalence, genetic heterogeneity, and mutation spectrum. *American Journal of Human Genetics*, 65(3), 664–670. <https://doi.org/10.1086/302553>

Carlsson, L., & Lazarides, E. (1983). ADP-ribosylation of the Mr 83,000 stress-inducible and glucose-regulated protein in avian and mammalian cells: Modulation by heat shock and glucose starvation. *Proceedings of the National Academy of Sciences of the United States of America*, 80(15), 4664–4668. <https://doi.org/10.1073/pnas.80.15.4664>

Catchen, J. M., Amores, A., Hohenlohe, P., Cresko, W., & Postlethwait, J. H. (2011). Stacks: Building and genotyping loci de novo from short-read sequences. *G3: Genes|Genomes|Genetics*, *1*(3), 171–182. <https://doi.org/10.1534/g3.111.000240>

Chang, A. C., & Cohen, S. N. (1974). Genome construction between bacterial species in vitro: Replication and expression of Staphylococcus plasmid genes in Escherichia coli. *Proceedings of the National Academy of Sciences of the United States of America*, *71*(4), 1030–1034. <https://doi.org/10.1073/pnas.71.4.1030>

Chevalier, M., King, L., Wang, C., Gething, M. J., Elguindi, E., & Blond, S. Y. (1998). Substrate binding induces depolymerization of the C-terminal peptide binding domain of murine GRP78/BiP. *Journal of Biological Chemistry*, *273*(41), 26827–26835. <https://doi.org/10.1074/jbc.273.41.26827>

Crouzier, L., Richard, E. M., Sourbron, J., Lagae, L., Maurice, T., & Delprat, B. (2021). Use of zebrafish models to boost research in rare genetic diseases. *International Journal of Molecular Sciences*, *22*(24), 13356. <https://doi.org/10.3390/ijms222413356>

De Los Rios, P., Ben-Zvi, A., Slutsky, O., Azem, A., & Goloubinoff, P. (2006). Hsp70 chaperones accelerate protein translocation and the unfolding of stable protein aggregates by entropic pulling. *Proceedings of the National Academy of Sciences of the United States of America*, *103*(16), 6166–6171. <https://doi.org/10.1073/pnas.0510496103>

Duennwald, M. L., Echeverria, A., & Shorter, J. (2012). Small heat shock proteins potentiate amyloid dissolution by protein disaggregases from yeast and humans. *PLoS Biology*, *10*(6), e1001346. <https://doi.org/10.1371/journal.pbio.1001346>

Ellis, R. J. (1990). The molecular chaperone concept. *Seminars in Cell Biology*, *1*(1), 1–9.

Er, E., Oliver, L., Cartron, P.-F., Juin, P., Manon, S., & Vallette, F. M. (2006). Mitochondria as the target of the pro-apoptotic protein Bax. *Biochimica et Biophysica Acta (BBA) - Bioenergetics*, *1757*(9–10), 1301–1311. <https://doi.org/10.1016/j.bbabi.2006.05.032>

Fernández-Fernández, M. R., & Valpuesta, J. M. (2018). Hsp70 chaperone: A master player in protein homeostasis. *F1000Research*, 7, F1000 Faculty Rev-1497. <https://doi.org/10.12688/f1000research.15528.1>

Flaherty, K. M., DeLuca-Flaherty, C., & McKay, D. B. (1990). Three-dimensional structure of the ATPase fragment of a 70K heat-shock cognate protein. *Nature*, 346(6285), 623–628. <https://doi.org/10.1038/346623a0>

Flynn, G. C., Chappell, T. G., & Rothman, J. E. (1989). Peptide binding and release by proteins implicated as catalysts of protein assembly. *Science*, 245(3859), 385–390. <https://doi.org/10.1126/science.2773615>

Fourie, A. M., Sambrook, J. F., & Gething, M. J. (1994). Common and divergent peptide binding specificities of hsp70 molecular chaperones. *Journal of Biological Chemistry*, 269(41), 30470–30478. <https://doi.org/10.1074/jbc.269.41.30470>

Freiden, P. J., Gaut, J. R., & Hendershot, L. M. (1992). Interconversion of three differentially modified and assembled forms of BiP. *EMBO Journal*, 11(1), 63–70. <https://doi.org/10.1002/j.1460-2075.1992.tb05028.x>

Gao, X., Carroni, M., Nussbaum-Krammer, C., Mogk, A., Nillegoda, N. B., Szlachcic, A., Guilbride, D. L., Saibil, H. R., Mayer, M. P., & Bukau, B. (2015). Human Hsp70 disaggregase reverses Parkinson's-linked α -synuclein amyloid fibrils. *Molecular Cell*, 59(5), 781–793. <https://doi.org/10.1016/j.molcel.2015.07.012>

Gehrmann, M., Marienhagen, J., Eichholtz-Wirth, H., Fritz, E., Ellwart, J., Jäättelä, M., Zilch, T., & Multhoff, G. (2005). Dual function of membrane-bound heat shock protein 70 (Hsp70), Bag-4, and Hsp40: Protection against radiation-induced effects and target structure for natural killer cells. *Cell Death & Differentiation*, 12(1), 38–51. <https://doi.org/10.1038/sj.cdd.4401510>

Gething, M.-J. (1999). Role and regulation of the ER chaperone BiP. *Seminars in Cell & Developmental Biology*, 10(5), 465–472. <https://doi.org/10.1006/scdb.1999.0318>

Gorbatyuk, M. S., & Gorbatyuk, O. S. (2013). The molecular chaperone GRP78/BiP as a therapeutic target for neurodegenerative disorders: A mini review. *Journal of Genetic Syndromes & Gene Therapy*, 4(2), 128. <https://doi.org/10.4172/2157-7412.1000128>

Groth, C., Nornes, S., McCarty, R., Tamme, R., & Lardelli, M. (2002). Identification of a second presenilin gene in zebrafish with similarity to the human Alzheimer's disease gene presenilin2. *Development Genes and Evolution*, 212(10), 486–490. <https://doi.org/10.1007/s00427-002-0269-5>

Guerreiro, R. J., Baquero, M., Blesa, R., Boada, M., Brás, J. M., Bullido, M. J., Calado, A., Crook, R., Ferreira, C., Frank, A., Gómez-Isla, T., Hernández, I., Lleó, A., Machado, A., Martínez-Lage, P., Masdeu, J., Molina-Porcel, L., Molinuevo, J. L., Pastor, P., Pérez-Tur, J., Relvas, R., Oliveira, C. R., Ribeiro, M. H., Rogaeva, E., Sa, A., Samaranch, L., Sánchez-Valle, R., Santana, I., Tàrraga, L., Valdivieso, F., Singleton, A., Hardy, J., & Clarimón, J. (2010). Genetic screening of Alzheimer's disease genes in Iberian and African samples yields novel mutations in presenilins and APP. *Neurobiology of Aging*, 31(5), 725–731. <https://doi.org/10.1016/j.neurobiolaging.2008.06.012>

Guo, F., Rocha, K., Bali, P., Pranpat, M., Fiskus, W., Boyapalle, S., Kumaraswamy, S., Balasis, M., Greedy, B., Armitage, E. S., Lawrence, N., & Bhalla, K. (2005). Abrogation of heat shock protein 70 induction as a strategy to increase antileukemia activity of heat shock protein 90 inhibitor 17-allylamino-demethoxy geldanamycin. *Cancer Research*, 65(22), 10536–10544. <https://doi.org/10.1158/0008-5472.CAN-05-1799>

Haass, C., Kaether, C., Thinakaran, G., & Sisodia, S. (2012). Trafficking and proteolytic processing of APP. *Cold Spring Harbor Perspectives in Medicine*, 2(5), a006270. <https://doi.org/10.1101/cshperspect.a006270>

Hantschel, M., Pfister, K., Jordan, A., Scholz, R., Andreesen, R., Schmitz, G., Schmetzer, H., Hiddemann, W., & Multhoff, G. (2000). Hsp70 plasma membrane expression on primary tumor biopsy material and bone marrow of leukemic patients. *Cell Stress & Chaperones*, 5(5), 438–442. [https://doi.org/10.1379/1466-1268\(2000\)005<0438:hpmeop>2.0.co;2](https://doi.org/10.1379/1466-1268(2000)005<0438:hpmeop>2.0.co;2)

Hendershot, L. M., Ting, J., & Lee, A. S. (1988). Identity of the immunoglobulin heavy-chain-binding protein with the 78,000-dalton glucose-regulated protein and the role of

posttranslational modifications in its binding function. *Molecular and Cellular Biology*, 8(10), 4250–4256. <https://doi.org/10.1128/mcb.8.10.4250-4256.1988>

Kampinga, H. H., & Bergink, S. (2016). Heat shock proteins as potential targets for protective strategies in neurodegeneration. *Lancet Neurology*, 15(7), 748–759. [https://doi.org/10.1016/S1474-4422\(16\)00099-5](https://doi.org/10.1016/S1474-4422(16)00099-5)

Kampinga, H. H., & Craig, E. A. (2010). The HSP70 chaperone machinery: J proteins as drivers of functional specificity. *Nature Reviews Molecular Cell Biology*, 11(8), 579–592. <https://doi.org/10.1038/nrm2941>

Knarr, G., Gething, M. J., Modrow, S., & Buchner, J. (1995). BiP-binding sequences in antibodies. *Journal of Biological Chemistry*, 270(47), 27589–27594. <https://doi.org/10.1074/jbc.270.47.27589>

Krüger, J., Moilanen, V., Majamaa, K., & Remes, A. M. (2012). Molecular genetic analysis of the APP, PSEN1, and PSEN2 genes in Finnish patients with early-onset Alzheimer disease and frontotemporal lobar degeneration. *Alzheimer Disease & Associated Disorders*, 26(3), 272–276. <https://doi.org/10.1097/WAD.0b013e318231e6c7>

Kumar, S., & Hedges, S. (1998). A molecular timescale for vertebrate evolution. *Nature*, 392, 917–920. <https://doi.org/10.1038/31927>

Lajoie, P., & Snapp, E. L. (2011). Changes in BiP availability reveal hypersensitivity to acute endoplasmic reticulum stress in cells expressing mutant huntingtin. *Journal of Cell Science*, 124(19), 3332–3343. <https://doi.org/10.1242/jcs.087510>

Ledford, B. E., & Leno, G. H. (1994). ADP-ribosylation of the molecular chaperone GRP78/BiP. *Molecular and Cellular Biochemistry*, 138(1), 141–148. <https://doi.org/10.1007/BF00926449>

Lee, L. C., Chen, C. M., Chen, F. L., Lin, P. Y., Hsiao, Y. C., Wang, P. R., Su, M. T., Hsieh-Li, H. M., Hwang, J. C., Wu, C. H., Lee, G. C., Singh, S., Lin, Y., Hsieh, S. Y., Lee-Chen, G. J., & Lin, J. Y. (2009). Altered expression of HSPA5, HSPA8, and PARK7 in spinocerebellar ataxia type 17 identified by 2-dimensional fluorescence difference in gel

electrophoresis. *Clinical Chemistry and Laboratory Medicine*, 400(1-2), 56-62. <https://doi.org/10.1016/j.cca.2008.10.013>

Leimer, U., Lun, K., Romig, H., Walter, J., Grünberg, J., Brand, M., & Haass, C. (1999). Zebrafish (*Danio rerio*) presenilin promotes aberrant amyloid β -peptide production and requires a critical aspartate residue for its function in amyloidogenesis. *Biochemistry*, 38(41), 13602–13609. <https://doi.org/10.1021/bi991453n>

Leno, G. H., & Ledford, B. E. (1990). Reversible ADP-ribosylation of the 78 kDa glucose-regulated protein. *FEBS Letters*, 276(1), 29–33. [https://doi.org/10.1016/0014-5793\(90\)80967-K](https://doi.org/10.1016/0014-5793(90)80967-K)

Leustek, T., Toledo, H., Brot, N., & Weissbach, H. (1991). Calcium-dependent autophosphorylation of the glucose-regulated protein, Grp78. *Archives of Biochemistry and Biophysics*, 289(1), 256–261. [https://doi.org/10.1016/0003-9861\(91\)90469-Y](https://doi.org/10.1016/0003-9861(91)90469-Y)

Levy-Lahad, E., Wijisman, E. M., Nemens, E., Anderson, L., Goddard, K. A., Weber, J. L., Bird, T. D., & Schellenberg, G. D. (1995). A familial Alzheimer's disease locus on chromosome 1. *Science*, 269(5226), 970–973. <https://doi.org/10.1126/science.7638621>

Lieschke, G. J., & Currie, P. D. (2007). Animal models of human disease: Zebrafish swim into view. *Nature Reviews Genetics*, 8(5), 353–367. <https://doi.org/10.1038/nrg2091>

Mayer, M. P., & Gierasch, L. M. (2019). Recent advances in the structural and mechanistic aspects of Hsp70 molecular chaperones. *Journal of Biological Chemistry*, 294(6), 2085–2097. <https://doi.org/10.1074/jbc.REV118.002810>

Mayer, M. P., & Bukau, B. (2005). Hsp70 chaperones: cellular functions and molecular mechanism. *Cellular and Molecular Life Sciences*, 62(7), 670-684. <https://doi.org/10.1007/s00018-005-5171-5>

McKay, D. B. (1993). Structure and mechanism of 70-kDa heat-shock-related proteins. *Advances in Protein Chemistry*, 44, 67–98. [https://doi.org/10.1016/s0065-3233\(08\)60564-1](https://doi.org/10.1016/s0065-3233(08)60564-1)

Melo, E.P., T. Konno, I. Farace, M.A. Awadelkareem, L.R. Skov, F. Teodoro, T.P. Sancho, A.W. Paton, J.C. Paton, M. Fares, P.M.R. Paulo, X. Zhang, E. Avezov (2022) Stress-induced protein disaggregation in the endoplasmic reticulum catalysed by BiP. *Nature Commun.* 13: 2501. <https://doi.org/10.1038/s41467-022-30238-2>

Morrow, J. F., Cohen, S. N., Chang, A. C., Boyer, H. W., Goodman, H. M., & Helling, R. B. (1974). Replication and transcription of eukaryotic DNA in *Escherichia coli*. *Proceedings of the National Academy of Sciences of the United States of America*, 71(5), 1743–1747. <https://doi.org/10.1073/pnas.71.5.1743>

Muchowski, P. J., Schaffar, G., Sittler, A., Wanker, E. E., Hayer-Hartl, M. K., Hartl, F. U. (2000). Hsp70 and Hsp40 chaperones can inhibit self-assembly of polyglutamine proteins into amyloid-like fibrils. *Proceedings of the National Academy of Sciences of the United States of America*, 97(14), 7841-7846. <https://doi.org/10.1073/pnas.140202897>

Multhoff, G., & Hightower, L. E. (2011). Distinguishing integral and receptor-bound heat shock protein 70 (Hsp70) on the cell surface by Hsp70-specific antibodies. *Cell Stress and Chaperones*, 16(3), 251-255. <https://doi.org/10.1007/s12192-011-0317-4>

Multhoff, G., Botzler, C., Wiesnet, M., Müller, E., Meier, T., Wilmanns, W., & Issels, R. D. (1995). A stress-inducible 72-kDa heat-shock protein (HSP72) is expressed on the surface of human tumor cells, but not on normal cells. *International Journal of Cancer*, 61(2), 272-279. <https://doi.org/10.1002/ijc.2910610222>

Musa, A., Lehrach, H., & Russo, V. E. (2001). Distinct expression patterns of two zebrafish homologues of the human APP gene during embryonic development. *Developmental Genes and Evolution*, 211(8), 563-567. <https://doi.org/10.1007/s00427-001-0189-9>

Newman, M., Ebrahimie, E., & Lardelli, M. (2014). Using the zebrafish model for Alzheimer's disease research. *Frontiers in Genetics*, 5, 189. <https://doi.org/10.3389/fgene.2014.00189>

Lajoie, P., & Snapp, E. L. (2011). Changes in BiP availability reveal hypersensitivity to acute endoplasmic reticulum stress in cells expressing mutant huntingtin. *Journal of Cell Science*, 124(Pt 19), 3332–3343. <https://doi.org/10.1242/jcs.087510>

Nornes, S., Newman, M., Wells, S., Verdile, G., Martins, R. N., & Lardelli, M. (2009). Independent and cooperative action of Psen2 with Psen1 in zebrafish embryos. *Experimental Cell Research*, 315(16), 2791–2801. <https://doi.org/10.1016/j.yexcr.2009.06.023>

Perera, L. A., & Ron, D. (2023). AMPylation and endoplasmic reticulum protein folding homeostasis. *Cold Spring Harbor Perspectives in Biology*, 15(3), a041265. <https://doi.org/10.1101/cshperspect.a041265>

Persky, N. S., & Lovett, S. T. (2008). Mechanisms of recombination: lessons from *E. coli*. *Critical reviews in biochemistry and molecular biology*, 43(6), 347–370. <https://doi.org/10.1080/10409230802485358>

Pieri, L., Madiona, K., Bousset, L., & Melki, R. (2012). Fibrillar α -synuclein and huntingtin exon 1 assemblies are toxic to the cells. *Biophysical Journal*, 102(12), 2894–2905. <https://doi.org/10.1016/j.bpj.2012.04.050>

Pouyssegur, J., Shiu, R. P., & Pastan, I. (1977). Induction of two transformation-sensitive membrane polypeptides in normal fibroblasts by a block in glycoprotein synthesis or glucose deprivation. *Cell*, 11(4), 941–947. [https://doi.org/10.1016/0092-8674\(77\)90305-1](https://doi.org/10.1016/0092-8674(77)90305-1)

Preissler, S., Rato, C., Chen, R., Antrobus, R., Ding, S., Fearnley, I. M., & Ron, D. (2015). AMPylation matches BiP activity to client protein load in the endoplasmic reticulum. *eLife*, 4, e12621. <https://doi.org/10.7554/eLife.12621>

Radons, J. (2016). The human HSP70 family of chaperones: Where do we stand? *Cell Stress and Chaperones*, 21(3), 379–404. <https://doi.org/10.1007/s12192-016-0676-6>

Rogaev, E. I., Sherrington, R., Rogaeva, E. A., Levesque, G., Ikeda, M., Liang, Y., Chi, H., Lin, C., Holman, K., Tsuda, T., et al. (1995). Familial Alzheimer's disease in kindreds with missense mutations in a gene on chromosome 1 related to the Alzheimer's disease type 3 gene. *Nature*, 376(6543), 775–778. <https://doi.org/10.1038/376775a0>

Rosenzweig, R., Nillegoda, N. B., Mayer, M. P., & Bukau, B. (2019). The Hsp70 chaperone network. *Nature Reviews Molecular Cell Biology*, 20(11), 665-680. <https://doi.org/10.1038/s41580-019-0133-3>

Rüdiger, S., Germeroth, L., Schneider-Mergener, J., & Bukau, B. (1997). Substrate specificity of the DnaK chaperone determined by screening cellulose-bound peptide libraries. *The EMBO Journal*, 16(7), 1501-1507. <https://doi.org/10.1093/emboj/16.7.1501>

Schmid, D., Baici, A., Gehring, H., & Christen, P. (1994). Kinetics of molecular chaperone action. *Science*, 263(5149), 971-973. <https://doi.org/10.1126/science.8310296>

Sharma, S. K., De los Rios, P., Christen, P., Lustig, A., & Goloubinoff, P. (2010). The kinetic parameters and energy cost of the Hsp70 chaperone as a polypeptide unfoldase. *Nature Chemical Biology*, 6(12), 914-920. <https://doi.org/10.1038/nchembio.455>

Sherrington, R., Froelich, S., Sorbi, S., Campion, D., Chi, H., Rogaeva, E. A., Levesque, G., Rogaev, E. I., Lin, C., Liang, Y., Ikeda, M., Mar, L., Brice, A., Agid, Y., Percy, M. E., Clerget-Darpoux, F., Piacentini, S., Marcon, G., Nacmias, B., Amaducci, L., Frebourg, T., Lannfelt, L., Rommens, J. M., & St George-Hyslop, P. H. (1996). Alzheimer's disease associated with mutations in presenilin 2 is rare and variably penetrant. *Human Molecular Genetics*, 5(7), 985-988. <https://doi.org/10.1093/hmg/5.7.985>

Sherrington, R., Rogaev, E. I., Liang, Y., Rogaeva, E. A., Levesque, G., Ikeda, M., Chi, H., Lin, C., Li, G., Holman, K., Tsuda, T., Mar, L., Foncin, J. F., Bruni, A. C., Montesi, M. P., Sorbi, S., Rainero, I., Pinessi, L., Nee, L., Chumakov, I., Pollen, D., Brookes, A., Sanseau, P., Polinsky, R. J., Wasco, W., Da Silva, H. A., Haines, J. L., Pericak-Vance, M. A., Tanzi, R. E., Roses, A. D., Fraser, P. E., Rommens, J. M., & St George-Hyslop, P. H. (1995). Cloning of a gene bearing missense mutations in early-onset familial Alzheimer's disease. *Nature*, 375(6534), 754-760. <https://doi.org/10.1038/375754a0>

Smith H. O. (1979). Nucleotide sequence specificity of restriction endonucleases. *Science* (New York, N.Y.), 205(4405), 455-462. <https://doi.org/10.1126/science.377492>

Sousa, R., Liao, H. S., Cuéllar, J., Jin, S., Valpuesta, J. M., Jin, A. J., & Lafer, E. M. (2016). Clathrin-coat disassembly illuminates the mechanisms of Hsp70 force generation. *Nature Structural & Molecular Biology*, 23(9), 821-829. <https://doi.org/10.1038/nsmb.3272>

Stankiewicz, A. R., Lachapelle, G., Foo, C. P., Radicioni, S. M., & Mosser, D. D. (2005). Hsp70 inhibits heat-induced apoptosis upstream of mitochondria by preventing Bax translocation. *Journal of Biological Chemistry*, 280(46), 38729-38739. <https://doi.org/10.1074/jbc.M509497200>

Swain, J. F., Dinler, G., Sivendran, R., Montgomery, D. L., Stotz, M., & Gierasch, L. M. (2007). Hsp70 chaperone ligands control domain association via an allosteric mechanism mediated by the interdomain linker. *Molecular Cell*, 26(1), 27-39. <https://doi.org/10.1016/j.molcel.2007.02.020>

Taylor, I. R., Ahmad, A., Wu, T., Nordhues, B. A., Bhullar, A., Gestwicki, J. E., & Zuiderweg, E. R. P. (2018). The disorderly conduct of Hsc70 and its interaction with the Alzheimer's-related Tau protein. *Journal of Biological Chemistry*, 293(27), 10796-10809. <https://doi.org/10.1074/jbc.RA118.002234>

Voisin, T., & Vellas, B. (2009). Diagnosis and treatment of patients with severe Alzheimer's disease. *Drugs & Aging*, 26(2), 135-144. <https://doi.org/10.2165/0002512-200926020-00005>

Wang, J. L., Liem, D., & Ping, P. (2017). HSPA5 gene encoding Hsp70 chaperone BiP in the endoplasmic reticulum. *Gene*, 618, 14-23. <https://doi.org/10.1016/j.gene.2017.03.005>

Wentink, A. S., Nillegoda, N. B., Feufel, J., Ubartaitè, G., Schneider, C. P., De Los Rios, P., Hennig, J., Barducci, A., & Bukau, B. (2020). Molecular dissection of amyloid disaggregation by human HSP70. *Nature*, 587(7834), 483-488. <https://doi.org/10.1038/s41586-020-2904-6>

Wentink, A., Nussbaum-Krammer, C., & Bukau, B. (2019). Modulation of amyloid states by molecular chaperones. *Cold Spring Harbor Perspectives in Biology*, 11(7), a033969. <https://doi.org/10.1101/cshperspect.a033969>

Yang, J., Nune, M., Zong, Y., Zhou, L., & Liu, Q. (2015). Close and allosteric opening of the polypeptide-binding site in a human Hsp70 chaperone BiP. *Structure*, 23(12), 2191-2203. <https://doi.org/10.1016/j.str.2015.10.012>

Zhang, H., Hu, H., Wu, S., & Perrett, S. (2023). Effect of evolution of the C-terminal region on chaperone activity of Hsp70. *Protein Science*, 32(1), e4549. <https://doi.org/10.1002/pro.4549>

Zhao, F. G., Wang, Y. H., Yang, J. F., Ma, Q. L., Tang, Z., Dong, X. M., & Chan, P. (2005). Association between acyl-coenzyme A: cholesterol acyltransferase gene and risk for Alzheimer's disease in Chinese. *Neuroscience Letters*, 388(1), 17-20. <https://doi.org/10.1016/j.neulet.2005.06.020>

Zhu, X., Zhao, X., Burkholder, W. F., Gragerov, A., Ogata, C. M., Gottesman, M. E., & Hendrickson, W. A. (1996). Structural analysis of substrate binding by the molecular chaperone DnaK. *Science*, 272(5260), 1606–1614. <https://doi.org/10.1126/science.272.5260.1606>

Zhuravleva, A., & Gierasch, L. M. (2015). Substrate-binding domain conformational dynamics mediate Hsp70 allostery. *Proceedings of the National Academy of Sciences U S A*, 112(22), E2865–E2873. <https://doi.org/10.1073/pnas.1506897112>

Zuiderweg, E. R., Hightower, L. E., & Gestwicki, J. E. (2017). The remarkable multivalency of the Hsp70 chaperones. *Cell Stress & Chaperones*, 22(2), 173–189. <https://doi.org/10.1007/s12192-017-0776-y>

ANNEXES

Annex A - Fw sequence of miniprep from ligation colony

```
Alignment of Sequence_1: [ORF zfiP_V25.xdna] with Sequence_2: [Sequence Window #8]
Similarity : 220/963 (22.85 %)

Seq_1 1      Gttgggacagtgattgggatcgacctcgggaccacatactcctgtgttgaggatctacaag 60
Seq_2 1      ----- 0

Seq_1 61     aatggccgtgttgagattattgccaatgaccagggaaaccgcatcactccgtcatacgtg 120
Seq_2 1      -----TTA 3

Seq_1 121    gcctttaccactgaaggagagcggtcatcggagatgctgcaagaaccagctcacatcc 180
Seq_2 4      A-CC-TATAAAATAGGCGTATCACGAGGCCCTTCGTCTTCACCTCGAGAAATCATAAAA 61

Seq_1 181    aacctgaaaaactgtgttgacgccaagaggctgatcggaacgacatggggcgactct 240
Seq_2 62     AATTTATTTGCTTTGTGAGCGGATAACAATTATAATAGATTCAATTGTGAGCGGATAACA 121

Seq_1 241    tctgtgcagcaggacatcaataacttcccctttaaggatgatgagaagaaaaaagcct 300
Seq_2 122    ATTTCACACAGAATTCATTAAAGAGGAGAAATTAAGTATGAGAGGATCTCACCATCAOCA 181

Seq_1 301    cacatccagctggacatcggctcctggtcagatgaagacgtttgcaccggaggaaattcc 360
Seq_2 182    TCACCATACGGATCCAGTAATGACCTCAGAACTCCATCTGGATTTGTTTCAGAACGCTGG 241

Seq_1 361    gccatggttttgaccaagatgaaggaaaccgagaggttatctgggaagaaggctcact 420
Seq_2 242    TTGCCGCCGGGCGTTTTTATTTGGTGGAGAAATCCAAGCTAGCTTGGCGAGATTTTCAGGAG 301

Seq_1 421    catgctgtggtcaccgttctcgtctatttcaacgatgctcagcgtcaggccactaaagat 480
Seq_2 302    CTAAGGAAGCTAAAATGGAGAAAAAATCACTGGATATACCACCGTTGATATATCCCAAT 361

Seq_1 481    gctggaaccattgctgggctgaatgcatgaggatcatcaatgacacctacggcggctgcc 540
Seq_2 362    GGCATCGTAAAGAACATTTTGGAGCATTTTCAGTCAGTTGCTCAATGTACCTATAACCAGA 421

Seq_1 541    attgcatacggcttgacaagaggacggagagaaaaacatcctggtgttcgatctgggt 600
Seq_2 422    CCGTTCAGCTGGATATTACGGCCCTTTTAAAGACCGTAAAGAAAAATAAGCACAAAGTTT 481

Seq_1 601    ggtggcacctttgacgtgtctctgctgaccatcgataaccggcgtgttgaagtgtggcc 660
Seq_2 482    ATCCGGCCCTTTATTCACATTCCTGCCCCGCTGATGAATGCTCATCCGGAATTTCTGATGG 541

Seq_1 661    acaaacggagacactcacctgggaggagaagacttcgaccagcgcgtcatggagcacttc 720
Seq_2 542    CAATGAAAGACGGGTGAGCTGGTGATATGGGATAGTGTTACCCCTTGTACACCGTTTTCC 601

Seq_1 721    atcaagctgtacaagaagaagacgggcaaacgctgcaagaacaaccgcccgtgcag 780
Seq_2 602    ATGAGCAAACCTGAAACGTTTTTCATCGCTCTGGAGTGAAATACCAACGACGATTTCCGGCAGT 661

Seq_1 781    aagctgcgcagagaggtggagaaggctaagagagcgtgtctgcccagcatcaggccgc 840
Seq_2 662    TTCTACACATATATTCGCAAGATGTGGCGTGTACGGTGAAAACTGGCCTATTTCCCTA 721

Seq_1 841    atcgagatcgagtcctctcttgaaggagaagatttctctgagactctcaccagagccaag 900
Seq_2 722    AAGGGTTTATTTGAGAATATGTTTTTCGTCTCAGCCAATCCCTGGGTGAGTTTCACCCAGTT 781

Seq_1 901    tttgaggagctcaacatggactgttccgctccactatgaagccggttcagaagttctg 960
Seq_2 782    TTGATTTAAACGTGGCCAATATGGACAACCTTTCGCCCCCGTTTTTCACCATGGGCAAAT 841

Seq_1 961    gaggactctgacccgaagaagccagatatogatgagatcgtgctggtcggcggtccact 1020
```

Seq_2	842	ATTATACGCAAGGCGACAAGGTGCTGATGCCGCTGGCGATTCAAGTTCATCATGCCGTTT	901
Seq_1	1021	cgtatcccgaagatccagcagctggggaaggagttcttcaacggaaaagagccgctccaga	1080
Seq_2	902	GTGATGGCTTCCATGTCGGCAGAAATGCTTAATGAATTACAACAGTACTGCCGATGAGTGGC	961
Seq_1	1081	ggaatcaaccctgaecgagggccgtggcgtaecggagetgctgtccaggetggagctctgtcc	1140
Seq_2	962	AG-----	963
Seq_1	1141	ggagaggaggagaccggatctggttcttctggacgtgtgtccgctgactctgggcatt	1200
Seq_2	964	-----	963
Seq_1	1201	gagactgttggaggagtgtgacccaaactcattcccagaaaactgttgtcccaccaag	1260
Seq_2	964	-----	963
Seq_1	1261	aaatcccagatcttctccactgettccgacaaccagcccaccgtcaactatcaaagttat	1320
Seq_2	964	-----	963
Seq_1	1321	gagggcgagcgtcccctgacccaaagacaaccatctgctgggcacctttgacctgacagge	1380
Seq_2	964	-----	963
Seq_1	1381	atccctccagcactcgtggtgtcccacagatcgaggttaactttcgagatcgacgtcaac	1440
Seq_2	964	-----	963
Seq_1	1441	ggcatcctgcgctcaccgcccgaagacaaggcaccggaaaacaaaaacaagatcaccatt	1500
Seq_2	964	-----	963
Seq_1	1501	accaacgaccagaaccggctgacccctgaggacatcgagagaatggtgaacgaagccgag	1560
Seq_2	964	-----	963
Seq_1	1561	agattcgtgatgaggacaagaaactgaaggagagaatcgacagccgcaatgaattggag	1620
Seq_2	964	-----	963
Seq_1	1621	agctacgcctattcctgaagaaccagatcgggataaagagaaattaggcggaaaagtta	1680
Seq_2	964	-----	963
Seq_1	1681	tcctctgaagacaaggaggccatcgagaaggcagtgaggagagaagatcgagtggctggag	1740
Seq_2	964	-----	963
Seq_1	1741	gcgcatcaggacgcgatctggaggaattccaggccaaaaagaaggagctggaggaggtg	1800
Seq_2	964	-----	963
Seq_1	1801	gtgcagcccatcgtcagcaaaactgtacggcagtgccggaggaccaccgctgaagaggcc	1860
Seq_2	964	-----	963
Seq_1	1861	gaagagaaggacgagctgtag	1881
Seq_2	964	-----	963

Annex B – Chromatogram

